University of Porto

Faculty of Engineering

Single-Column Modelling of the Atmospheric Boundary Layer for the Study of Turbulence Parameterization Schemes

Tobias Osswald

(MSc in Mechanical Engineering)

Dissertation submited to the University of Porto
in partial satisfaction of the requirements for the
degree of Master in Mechanical Engineering.

July 2018

This document was typeset with LaTeX using the **CVR** thesis template.

Abstract

A single-column computational solver was developed to simulate the atmospheric boundary layer, with the objective of analyzing turbulence parameterizations focusing neutral and stably-stratified atmospheric conditions. The model allowed for the prediction of temperature, wind speed and turbulent quantities while accounting for a constant pressure gradient and the Coriolis forces based on a geostrophic wind vector. The investigated turbulence models ranged from a simple mixing-length model to two prognostic equations parameterizations, namely k-ℓ, k-ϵ and k-ϵ-ℓ variations.

Simulations were made under two sets of conditions for the neutrally-stratified atmosphere. First solutions under a steady-state formulation were simulated, for which the observations from the Leipzig wind profile were used for comparison. Second a transient case was compared with LES data. The effect of considering static-stability over the neutrally-stratified surface layer was studied, resulting in realistic vertical profiles of turbulent viscosity and proving their importance for modelling of the neutral atmosphere. Certain models became viable with this consideration.

Lastly, a stably-stratified boundary layer was simulated and compared against the results from the GABLS1 model inter-comparison study. Of all models the k-ℓ model, to which a simple modification was made to account for stability, provided the best results. The relative error for this model was found to be lower than 15%. Proposals for the improvement of the studied parameterizations were given.

Resumo

Foi desenvolvido um código computacional para um modelo de coluna vertical cuja função foi a simulação da camada limite atmosférica. O objetivo foi a análise de diferentes modelos de turbulência focando condições atmosféricas de estratificação neutra e estável. O modelo permitiu a previsão de temperatura, velocidade do vento e quantidades turbulentas. Teve-se em conta um gradiente de pressão constante e as forças de Coriolis através de um vetor de vento geostrófico. Os modelos de turbulência investigados compreenderam desde um simples modelo de comprimento de mistura a parametrizações de duas equações prognosticas, nomeadamente variações dos modelos k-ℓ, k-ϵ e k-ϵ-ℓ.

Para o caso da atmosfera com estratificação neutra foram feitas simulações com dois conjuntos de condições. Primeiro foram calculados os resultados numa formulação em regime permanente, para os quais foi utilizado o perfil de vento de Leipzig como comparação. O segundo foi um caso transiente, para o qual foram utilizados dados de um modelo LES. O efeito da consideração da estabilidade estática sobre a camada limite com estratificação neutra foi estudado tendo resultado em perfis verticais de viscosidade turbulenta realistas e provando a sua importância para a modelação da atmosfera neutra. Alguns modelos tornaram-se viáveis com esta consideração.

Finalmente uma camada limite atmosférica foi simulada e comparada com os resultados do estudo comparativo de modelos, GABLS1. De todos os modelos o k-ℓ, ao qual foi aplicada uma simples alteração para ter em conta a estabilidade, produziu os melhores resultados. O erro relativo deste modelo foi inferior a 15%. Propostas para o melhoramento das parametrizações estudadas foram dadas.

Contents

List of Figures

List of Tables

Nomenclature

Acronyms

ABL	Atmospheric Boundary Layer
GABLS	GEWEX Amospheric Boundary Layer Study
GEWEX	Global Energy and Water Cycle Experiment
LES	Large-Eddy Simulation
MOST	Monin-Obukhov Similarity Theory
NSE	Navier-Stokes Equations
SL	Surface Layer
TKE	Turbulence Kinetic Energy

Greek symbols

α	Thermal diffusivity	$L^2\,T^{-1}$
α_t	Turbulent thermal diffusivity	$L^2\,T^{-1}$
Γ	Diffusion coefficient	
κ	von Kàrmàn constant	
λ	Boundary-layer limiting length scale	L
μ	Fluid dynamic viscosity	$M\,L^{-1}\,T^{-1}$
ν	Fluid kinematic viscosity	$L^2\,T^{-1}$
ν_t	Turbulent viscosity	$L^2\,T^{-1}$
Ω	Earth's rotation rate	T^{-1}
ϕ_m, ϕ_h	Dimensionless velocity and temperature vertical profiles	
ϕ'	Latitude coordinate	
ψ_m, ψ_h	Surface-layer functions for boundary-layer wall-laws	
ϵ	Turbulence kinetic energy dissipation	$L^2\,T^{-3}$

ρ	Fluid density	$M\,L^{-3}$
σ_k, σ_ϵ	Turbulent Prandtl numbers for turbulent quantities	
θ_*	Surface-layer temperature turbulent scale	Θ
θ	Potential temperature	Θ
θ_0	Temperature reference field	Θ

Dimensionless parameters

Pr	Turbulent Prandtl number
Pr_n	Turbulent Prandtl number in neutrally-stratified conditions
Rb	Richardson bulk number
Rf	Richardson flux number
Ri	Richardson gradient number
Ro	Rossby number

Roman symbols

c_p	Isobaric specific heat capacity	$L^2\,T^{-2}\,\Theta^{-1}$
f	Coriolis frequency	T^{-1}
$\vec{G}$	Geostrophic wind velocity vector	$L\,T^{-1}$
$\vec{g}$	Gravity acceleration vector	$L\,T^{-2}$
k	Turbulence kinetic energy	$L^2\,T^{-2}$
ℓ	Mixing length	L
ℓ_ϵ	Dissipation length	L
$\mathcal{L}$	Obukhov length	L
N	Brunt-Väisälä frequency	T^{-1}
p	Fluid pressure	$M\,L^{-1}\,T^{-2}$
$\mathbb{P}$	Turbulence production term	$L^3\,T^{-4}$
R	Specific gas constant for dry air	$L^2\,T^{-2}\,\Theta^{-1}$
t	Time coordinate	T
T	Temperature	Θ
$\mathbf{T}$	Stress tensor	$M\,L^{-1}\,T^{-2}$
u_*	Surface-layer friction velocity	$L\,T^{-1}$

$\vec{v} = \{v_x, v_y, v_z\}$	Velocity field in vector form and x, y and z components	$L\,T^{-1}$
$\vec{x} = \{x, y, z\}$	Position vector and spatial coordinates	L
z_0, z_{m0}, z_{h0}	Aerodynamic roughness lengths	L

Sub- and superscripts

$_0$	Related to the SL
$_b$	Bottom cell face
$_B$	Bottom cell node
$_i$	Node index
$_j$	Time index
$_n$	Highest node index
$_P$	Central cell node
$_r$	Reference for the field variable
$_t$	Top cell face
$_T$	Top cell node

Other symbols

δ	Infinitesimal differential or element
$\nabla \cdot (\ )$	Divergence operator
$D \cdot (\ )/Dt$	Total or material derivative operator
∇	Gradient operator
$(\ ) \times (\ )$	Cross product operation
$(\ ) \cdot (\ )$	Inner product operation
$(\ ) \otimes (\ )$	Tensor product operation

Chapter 1

Introduction

The atmospheric boundary layer (ABL) has been the subject of several theoretical and experimental studies, given its importance for the understanding and prediction of meteorological phenomena. The fact that it is not yet a closed topic lies in its complexity, the influence of temperature gradients, moisture, cloud coverage, the Coriolis force responsible for the usual rotating flows around high and low-pressure areas and other parameters. This means that the more common well documented methods used for solving typical mechanical engineering flows, like the k-ϵ model, are not able to provide accurate descriptions without some modification; *e.g.*, Detering and Etling (1985) or Duynkereke (1988).

In order to better understand the ABL several simplifications have been done by Detering and Etling (1985), Duynkereke (1988) or Freedman and Jacobson (2002) among others to analyze the influence that individual parameters have on it. One such simplification often used is that the properties of the atmosphere show negligible changes with the four cardinal directions. This results in a single column model. In order to remove the effects of buoyancy that lead to an increase or decrease of turbulence, the evolution of temperature of the ABL must be such that it leads to what is known as neutral stratification. Finally, both the horizontal pressure gradient driving the wind and density are often assumed as constant over its height resulting in a barotropic atmosphere.

These conditions are rare in the ABL and even more rarely registered given that measurements over its 400 to 2000 m require great effort. Mildner (1932) made such an effort using weather balloons and measuring their speed throughout their ascent when the conditions of a barotropic, neutral, horizontally homogeneous atmosphere were met. Lettau (1950) later re-examined his discoveries and Blackadar (1962) then used this new information to infer an expression for a characteristic mixing length and its variation over height. This led to a better parameterization of turbulence models that make use of this parameter such as the one suggested by Apsley and Castro (1997). However, Detering and Etling (1985) showed that the measurements made by Mildner (1932) were not taken under a truly neutral atmosphere and stressed the fact that such conditions were very hard to encounter. When the equation given by Blackadar (1962) is the sole parameter used for the parameterization of turbulence the model is unable to respond to any conditions other then the ones specified previously. Djolov (1973) attempted an alteration to account for the stability of the ABL, although it is still somewhat inflexible as will be explained. If changes in topography are present other methods have to be used as pointed out by Beljaars *et al.* (1987).

Thus the necessity for a model with a higher order than just an equation prescribing the mixing length, led to several attempts at altering the standard k-ϵ model as introduced by Jones and Launder (1972). This model, has been used extensively to predict local geophysical flows such as Kitada (1987) where the movement of air in a coastal region is studied, though this leads to a sometimes inaccurate description of the real ABL Detering and Etling (1985). In this last article the authors suggested an alteration to the equation for the dissipation of the energy associated with turbulence or the turbulent kinetic energy (TKE), k, but their model did not predict the effects of stratification and was thus only adequate for neutral atmospheres. Duynkereke (1988) suggested another model that also included alterations to the TKE dissipation, ϵ, this time the effects of non-neutral stratification were contemplated. After that Apsley and Castro (1997) suggested limiting the mixing length in the k-ϵ model and Xu and Taylor (1997) reduced the importance of the highly experimental TKE dissipation equation by including the mixing length as defined by Blackadar (1962), thus creating a hybrid model. Duynkerke and Driedonks (1987) also suggested a model that made use of the k and ϵ parameters as well as the mixing length, but in their case using a formulation that accounted for stability. Several of the previous authors had realized the need for an alteration of the experimentally obtained constants required for the models and each had attempted in its own way to improve them. Freedman and Jacobson (2002) made an extensive study to these constants imposing theoretical limits and made some suggestions for their values. Venayagamoorthy and Stretch (2010) suggested a dependence on the local stratification for the Prandtl number, a parameter that is often set to a constant value.

Authors like Weng and Taylor (2003) or Holt and Raman (1988) used some of these models under the aforementioned conditions to review their accuracy and have a better understanding of their strengths and weaknesses. In recent years there has been an increase in joint efforts at developing an appropriate model for the ABL. This requires not only the models themselves but also observations with which to compare them. The GEWEX Atmospheric Boundary Layer Study (GABLS; GEWEX stands for the Global Energy and Water Cycle Experiment) projects were an effort to provide adequate data to test and benchmark ABL models. Since 2003 three phases were carried out. The GABLS1 consisted in the comparison of several single column models with the data provided by the generally more accurate but time-consuming large-eddy simulation (LES). These LES results were averaged and compared by Beare *et al.* (2006). Several single column model results were afterwards analyzed in Cuxart *et al.* (2006). For the GABLS2 data from the CASES-99 dataset consisting of extensive field-measurements of the ABL were used for the intercomparison. The data focused on two full diurnal cycles and the initial and boundary conditions for the computational flow solvers were established based on the observations. GABLS3 was again based on field measurements for a diurnal cycle, but the focus was on the prediction of both ABL and ground-surface thermal dynamics. This represents a further level of complexity as it requires the coupling of an atmospheric flow solver with a land-soil model to effectively predict the surface fluxes of momentum, energy and moisture.

The purpose of the present work was the development of a single-column ABL solver, *i.e.* a 1D model to solve for the vertical profiles of the relevant quantities. Such a model was then used for the testing of turbulence parameterizations, common to both geophysical and engineering fields. In the long term such code will allow for the analysis and development of parameterizations for the real ABL under conditions of thermal

stratification and Coriolis acceleration.

This thesis is divided into six parts. This first chapter explains the state of the art and the main objectives. In chapter two the governing equations are explained alongside the main turbulence models. Chapter three explains how the equations were discretized and solved. The fourth chapter deals with the neutral atmosphere. The models are first presented, results for steady-state and transient simulations are presented and afterwards analyzed. The effect of stratification is then investigated. Chapter five follows an analogous structure but for stable stratification. The last chapter presents the conclusions.

Chapter 2

Governing Equations

In this chapter the fundamental equations and mathematical models are presented.

2.1 Fundamental Conservation Laws

The continuity equation ensures the conservation of mass,

$$\frac{\partial \rho}{\partial t} + \nabla \cdot (\rho \vec{v}) = 0\,. \tag{2.1}$$

Since the problem at hand is horizontally homogeneous, meaning that its conditions do not change with the four cardinal directions, the derivatives of velocities and densities in x and y are zero. Furthermore it shall be assumed that the average vertical wind speed (subsidence) is negligible. With these considerations in mind one can look at the continuity equation and realize that there is no variation of density over time,

$$\frac{\partial \rho}{\partial t} + \cancelto{0}{\frac{\partial \rho v_x}{\partial x}} + \cancelto{0}{\frac{\partial \rho v_y}{\partial y}} + \cancelto{0}{\frac{\partial \rho v_z}{\partial z}} = 0\,, \tag{2.2}$$

or vice versa the variation of density over time can be disregarded which results in a negligible subsidence.

For future reference the material derivative of a volume element is given as follows:

$$\rho \frac{D\vec{v}}{Dt} = \rho \left[\frac{\partial \vec{v}}{\partial t} + v_x \frac{\partial \vec{v}}{\partial x} + v_y \frac{\partial \vec{v}}{\partial y} + v_z \frac{\partial \vec{v}}{\partial z} \right] \Rightarrow \rho \frac{D\vec{v}}{Dt} = \rho \frac{\partial \vec{v}}{\partial t} + \rho (\vec{v} \cdot \nabla) \vec{v}\,. \tag{2.3}$$

Now the continuity equation may be manipulated and, being equivalent to zero, added to the material derivative,

$$\rho \frac{D\vec{v}}{Dt} = \rho \frac{D\vec{v}}{Dt} + \vec{v} \left[\frac{\partial \rho}{\partial t} + \rho (\nabla \cdot \vec{v}) + \vec{v} \cdot (\nabla \rho) \right] = \frac{\partial \vec{v} \rho}{\partial t} + \nabla \cdot (\rho \vec{v} \otimes \vec{v})\,. \tag{2.4}$$

Currently only the x and y directions are of interest and since ρ does not vary parallel to the ground the equations can be simplified even further so that the following is true for the first two vector components:

$$\frac{D\vec{v}}{Dt} = \frac{\partial \vec{v}}{\partial t} + \nabla \cdot (\vec{v} \otimes \vec{v})\,. \tag{2.5}$$

2.1.1 Momentum Balance

If Newton's second law of motion is applied to a small parcel of air with a mass δm and an acceleration $D\vec{v}/Dt$ the resultant forces applied to it are,

$$\delta\vec{F} = \delta m \frac{D\vec{v}}{Dt}. \tag{2.6}$$

It is now possible to apply this law to a small control volume with sides $\delta x\delta y\delta z$ fixed in space if the momentum entering through its faces is taken into account. In that case the mass is defined as,

$$\delta m = \rho\, \delta V = \rho\, \delta x\delta y\delta z\,. \tag{2.7}$$

The acceleration will include a convective term so that the general equation becomes,

$$\delta\vec{F} = \rho \frac{D\vec{v}}{Dt}\, \delta x\delta y\delta z\,. \tag{2.8}$$

2.1.2 Sum of Forces

As for the first term on equation (2.8), $\delta\vec{F}$ is a sum of several forces. Only the x and y directions will be considered since there is no need to calculate the vertical wind speed component that is zero. Gravity will be considered to ensure universality. The first term is due to the pressure gradient that has a resultant force perpendicular to the faces of the control volume so that the resultant force in the direction of x is given by $-\partial p/\partial x\, \delta x\delta y\delta z\,$.

Applying the same line of thought for the other coordinates the following equations for the pressure forces are obtained,

$$\delta\vec{F_p} = -\nabla p\, \delta x\delta y\delta z\,. \tag{2.9}$$

The second component of δF to be taken into account is a result of the viscosity of the fluid. In this case it will be assumed that the pressure gradients are not strong enough so as to require a compressible viscosity model. The stress tensor is given by the following expression as first derived by Stokes in 1845 (Acheson, 1990):

$$\mathbf{T} = \mu[\nabla\vec{v} + (\nabla\vec{v})^T] - 2/3\, \mu \cancelto{=0}{(\nabla\cdot\vec{v})}\mathbf{I}. \tag{2.10}$$

Having assumed incompressibility and a constant dynamic viscosity the resultant forces due to friction in each direction are written as

$$\delta F_t = \nabla\cdot\mathbf{T}\, \delta x\delta y\delta z\,. \tag{2.11}$$

For this case in particular and most cases related to meteorology there is yet another force that has to be taken into account upon the elaboration of the fundamental equations. The Coriolis force that acts on every moving particle inside a rotating system, *e.g.*

the earth. Following Arya (2001), the vertical component of this force is much smaller than the buoyancy forces and those resulting from the pressure gradient. The horizontal component, however, cannot be overlooked. If a vector $\vec{f}$ is defined with one component in z as $f = 2\,\Omega \sin\phi^{'}$, being Ω the earth's rotational speed and $\phi^{'}$ the latitude of the region being studied, the Coriolis force acting on a small volume of fluid can be defined as

$$\delta F_c = \rho\,(\vec{v} \times \vec{f})\,\delta x \delta y \delta z\,. \tag{2.12}$$

2.1.3 Geostrophic Wind and the Pressure Gradient

By summing all of the external forces including gravity, equaling them to the inertial term and then dividing by the volume $\delta x \delta y \delta z$, the Navier-Stokes equations (NSE) with the Coriolis term are obtained (Acheson, 1990),

$$\rho \frac{D\vec{v}}{Dt} = -\nabla p + \rho\,(\vec{v} \times \vec{f}) + \nabla \cdot \mathbf{T} + \rho\vec{g} \tag{2.13}$$

It is important to define the concept of geostrophic wind. Outside of the ABL where there are no surface effects and therefore no shearing stress the Coriolis force will equal the force generated by the pressure gradient. When this happens the wind is said to be geostrophic with a speed $\vec{G}$, so that

$$\rho(\vec{G} \times \vec{f}) = \nabla p\,. \tag{2.14}$$

If the assumption of a barotropic atmosphere is made, then the pressure gradient does not change with height, which means that this relation is valid for the whole ABL. Being so, it can be substituted into the NSE to give, after some mathematical manipulation,

$$\rho \frac{D\vec{v}}{Dt} = \rho\,(\vec{v} - \vec{G}) \times \vec{f} + \nabla \cdot \mathbf{T} + \rho\vec{g}\,. \tag{2.15}$$

This relation between the Coriolis force and the pressure gradient can also be interpreted graphically from the balance of the external forces applied to the control volume.

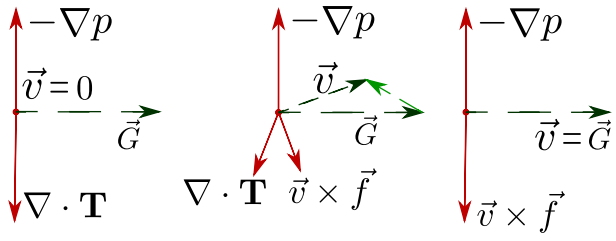

Figure 2.1: Balance of external forces for the ABL: Left to right; on the ground, in the center of the ABL, above the ABL.

It is important to remember that this last step was made assuming no inertial forces for the balance of the geostrophic wind. This is not entirely true if the geostrophic wind is changing but nonetheless acceptable and greatly simplifies the equations by removing the necessity of a further equation for the pressure. The pressure distribution is thus given in terms of velocity. By choosing a constant $\vec{G}$ a pressure gradient that is constant with height will be created. The equations are valid for a barotropic atmosphere only.

2.1.4 Heat Balance

The First Law of Thermodynamics can be applied to the control volume to yield an equation for the temperature. In this case like in many others related to meteorology an alternative variable to the temperature will be used, namely the potential temperature. This is the temperature that an air parcel would have if it were brought down adiabatically to the reference pressure of 1000 mbar. Being so, an adiabatic atmosphere would have a constant potential temperature which simplifies the equations and removes the need to account for the vertical pressure variation in the terms involving this new variable. Following Arya (2001) its definition is:

$$\theta = T \cdot \left(\frac{p_0 0}{p} \right)^{R/c_p}, \tag{2.16}$$

being R the specific gas constant, c_p the specific heat at constant pressure and $p_0 0 = 10^5$ Pa as the pressure at sea level. For the dry air case the small change of c_p with temperature or pressure does not require any special treatment and is assumed constant. Since the effect of moisture in the boundary-layer will not be considered, a simplification that does not reflect the more common situation in the ABL but that still allows for a study of several phenomena and variables in it, the potential temperature is enough to describe the thermodynamic state of the air and the virtual potential temperature which would include the influence of moisture is not required. The pressure can be obtained from its hydrostatic relation.

A general balance of heat fluxes in the control volume can be written as Stull (1988),

$$\rho c_p \frac{\partial \theta}{\partial t} + \rho c_p \, \vec{v} \cdot \nabla \theta = \nabla \cdot (\Gamma_h \, \nabla \theta) + R + L \,, \tag{2.17}$$

where Γ_h is the thermal conductivity. The first term accounts for the storage of heat over time, the second is due to the mass flux into and out of the control volume, the third term stands for the effect of conduction, prior measurement data has shown that this can be neglected (Stull, 1988) as well as the last two components, R and L, respectively the radiation and latent heat. Radiation is small when compared to the effects of mixing and turbulence (it may become important if clouds are present). As for the latent heat it corresponds to the energy released by evaporation or condensation being zero if these do not occur. The conduction is equally negligible when compared to the other heat transfer modes except near the ground where molecular transfer of both momentum and heat become significant.

With these simplifications the First Law can be rewritten as,

$$\frac{\partial \theta}{\partial t} = -\vec{v} \cdot \nabla \theta \,. \tag{2.18}$$

2.2 Reynolds Averaging

Although the equations that were deduced in the previous section are enough to describe the phenomenon accurately, it is necessary to account for turbulence in a way that

allows these equations to be solved numerically. This will be achieved by the Reynolds decomposition in which the variables are divided into an instantaneous average and a fluctuation.

$$\vec{v} = \overline{\vec{v}} + \vec{v'} \qquad \rho = \overline{\rho} + \rho' \qquad \theta = \overline{\theta} + \theta' \tag{2.19}$$

As for the fluctuation of ρ the Boussinesq hypothesis is used so that it is only relevant when associated with gravity. However, since the only relevant equations are in the x and y direction such is unimportant, except for some parameterizations regarding turbulence production that will be presented later on.

In geophysical flows, given the impossibility of repeating measurements, the average quantities are defined as temporal averages. Mathematically this is defined as

$$\overline{\phi} = \frac{1}{T}\int_{T} \phi(t)\, dt\,. \tag{2.20}$$

Beginning with the inertial term of the NSE – the material derivative, defined in equation (2.5) – equation (2.19) is substituted into it and one obtains

$$\rho\frac{D\vec{v}}{Dt} \equiv \rho\left[\frac{\partial(\overline{\vec{v}} + \vec{v'})}{\partial t} + \nabla\cdot(\overline{\vec{v}}\otimes\overline{\vec{v}}) + \nabla\cdot(\overline{\vec{v}}\otimes\vec{v'}) + \nabla\cdot(\vec{v'}\otimes\overline{\vec{v}}) + \nabla\cdot(\vec{v'}\otimes\vec{v'})\right] \tag{2.21}$$

Now the average is taken on both sides while minding that the average of the fluctuations is zero and the average of an average remains unchanged.

$$\overline{\rho\frac{D\overline{\vec{v}}}{Dt}} \equiv \rho\left[\frac{\partial\overline{\vec{v}}}{\partial t} + \nabla\cdot(\overline{\vec{v}}\otimes\overline{\vec{v}}) + \nabla\cdot\overline{(\vec{v'}\otimes\vec{v'})}\right] \tag{2.22}$$

Looking at the viscosity term from (2.15) and applying the same process,

$$\overline{\nabla\cdot\mu[\nabla\vec{v} + (\nabla\vec{v})^T]} = \nabla\cdot\mu[\nabla\overline{\vec{v}} + (\nabla\overline{\vec{v}})^T] \tag{2.23}$$

This happens because the fluctuation terms are isolated when their gradient is taken and therefore vanish when averaged. Doing the same for all other terms in the NSE, the following Reynolds averaged NSE can be derived,

$$\rho\left[\frac{\partial\overline{\vec{v}}}{\partial t} + \nabla\cdot(\overline{\vec{v}}\otimes\overline{\vec{v}}) + \nabla\cdot\overline{(\vec{v'}\otimes\vec{v'})}\right] = \rho(\overline{\vec{v}} - \vec{G})\times\vec{f} + \nabla\cdot\mu[\nabla\overline{\vec{v}} + (\nabla\overline{\vec{v}})^T] + \rho\vec{g} \tag{2.24}$$

Even though the effects of molecular viscosity are very small when compared to those of turbulent viscosity so that they could be neglected, they are still accounted for in the Reynolds stresses ($\overline{v_i'v_j'}$) for numerical stability. With the assumptions of horizontal homogeneity and no subsidence the equation in the x direction is

$$\frac{\partial\overline{v_x}}{\partial t} = f\,(\overline{v_y} - G_y) - \frac{\partial}{\partial z}\overline{v_x'v_z'} \tag{2.25}$$

and similarly in the y direction

$$\frac{\partial \overline{v_y}}{\partial t} = -f\left(\overline{v_x} - G_x\right) - \frac{\partial}{\partial z}\overline{v_y' v_z'} \tag{2.26}$$

A very similar manipulation is done to the heat equation. By making the Reynolds decomposition and then taking the average equation (2.18) is further manipulated with the continuity equation to give,

$$\frac{\partial \overline{\theta}}{\partial t} = -\frac{\partial \overline{\theta' v_z'}}{\partial z}\,. \tag{2.27}$$

Turbulent motions are part of the nature of atmospheric flows and Reynolds averaging allows these motions to be linked with the covariances of wind velocity and temperature. To solve such a flow, the question becomes on how these covariances can be computed, so that the set of equations becomes closed.

2.3 Turbulence Modelling

Given the large length scales on the order of hundreds of meters involved in the ABL associated with the velocity scales of around ten meters per second a quick analysis leads to quite large Reynolds numbers on the order of 50×10^6. This indicates that the effects of viscosity are small compared to the momentum of the fluid which is usually associated with turbulent flows. Many measurements have indeed shown that the ABL is strongly influenced by turbulent effects, so much so, that the molecular viscosity and conduction are negligible compared to the heat or momentum transfer through turbulence (Stull, 1988).

The equations developed previously regarding the balance of momentum and heat transfer already took this into account, however they are not enough to totally describe the problem since the covariances $\overline{v_i' v_j'}$ or $\overline{v_z' \theta'}$ are not known variables. In order to understand how these can be modeled a good understanding of the turbulent phenomena is required and many models have been suggested to solve for these variables. Some models introduce new variables as higher order covariances of the type $\overline{v_i v_j v_k}$ and these too require modeling which leads to an apparently endless set of equations to solve the problem of turbulence. Usually the problem is truncated by parameterization of higher order variables, but this approximation requires measurements for the determination of certain constants, exponentials or other unknowns and in certain cases where these are not mensurable the values that yielded the best results are chosen. These approximations lack any physical meaning and may result in a lack of accuracy, which is why higher order models that use more physical models and parameterizations only on higher order variables are usually better. The downside is the need to solve more equations, often differential, which leads to a higher demand on computational resources (Stull, 1988).

2.3.1 k-ϵ model

A common model of turbulence is the k-ϵ model that requires two equations, one for the turbulent kinetic energy (TKE represented here by k as is typical in mechanical

engineering applications although E is often used in meteorology) and another for the dissipation of TKE, ϵ.

One may achieve an intuitive understanding of this model by imagining a particle of fluid that is displaced by z' due to a turbulent fluctuation while at a temperature θ. If so it will enter the volume at $z + z'$, where z was its initial position, with a temperature that is warmer than the previous temperature of that control volume by $z' \, \partial\theta/\partial z$. Then it is safe to assume that the temperature fluctuation was $\theta' = z' \, \partial\theta/\partial z$. As for the difference in velocity with which the particle enters the volume it will be proportional to the difference between the speed it had at its initial position and the speed of the volume observed or $z' \, \partial|\vec{v}|/\partial z$. The proportionality constant will be named c so that $v_z' = c \, z' \, \partial|\vec{v}|/\partial z$.

By multiplying the two and taking an average $\overline{v_z'\theta'} = c \, \overline{z'^2} \, \partial|\vec{v}|/\partial z \, \partial\theta/\partial z$ can be written. It is obvious from this expression that the transfer of heat will be along the temperature gradient and proportional to a factor that includes the velocity gradient and some unknown variables. This expression is thus analogous to the one of molecular viscosity and so a parameter for the turbulent viscosity is created, ν_h. It is important to remember that this one is not a property of the fluid but of the flow since it depends on variables that are not easily determined as shown in the above expression. This turbulent viscosity can be different for different types of transfer be it momentum or heat transfer. Bearing these considerations in mind the following can be written for the second order momenta

$$\overline{v_x'v_z'} = -\nu_t \frac{\partial v_x}{\partial z}, \tag{2.28}$$

$$\overline{v_y'v_z'} = -\nu_t \frac{\partial v_y}{\partial z}, \tag{2.29}$$

$$\overline{\theta'v_z'} = -\nu_h \frac{\partial \theta}{\partial z}. \tag{2.30}$$

Usually a relation $\nu_t/\nu_h = \mathrm{Pr}$ is defined and can be held constant or dependent on flow characteristics. As is common in this closure problem the three unknown variables were replaced by new unknown variables.

This solution seems to agree with the physical nature of turbulence, however it relies on the simplification that the vortexes are small enough that the difference in a certain quantity is described correctly by the multiplication of their length by the derivative of this same quantity along the vertical axis. This is true only if the derivative does not change over the height of the vortex which is not entirely true for big vortexes as those caused by thermals. This means that the model will not describe the physics correctly under certain circumstances, such as strong instability, which may lead to odd parameterizations, *e.g.* a negative turbulent viscosity.

In order to determine the turbulent viscosity of the flow the definition of the Kolmogorov scales becomes very useful. Kolmogorov suggested that at very small scales where the dissipation of the TKE takes place turbulence is isotropic because at this level there have already been multiple vortex breakdowns so that the preferred flow directions from the larger scales have little impact. The Kolmogorov velocity scale is thus defined as $v_{kolmogorov} = \nu_t^{0.25} \, \epsilon^{0.25}$ and depends on the energy that crosses the small scales which is then dissipated ϵ and the turbulent viscosity ν_t (Arya, 2001; Detering and Etling, 1985).

As for the TKE it can be defined as

$$k = \frac{1}{2}(\overline{v'_x\, v'_x} + \overline{v'_y\, v'_y} + \overline{v'_z\, v'_z}). \tag{2.31}$$

So it is safe to assume that for an isotropic situation the TKE will be proportional to the square of the velocity fluctuations which are themselves proportional to the Kolmogorov velocity scale. After some algebraic manipulation this means that,

$$\nu_t = c_k \frac{k^2}{\epsilon}\,, \tag{2.32}$$

so a problem that once required a solution for the turbulent viscosity which was a vague parameter dependent on too many conditions now requires that the TKE and the TKE dissipation ϵ be discovered. The proportionality constant c_k like many other constants that are required for this model of turbulence is obtained through a mixture of physical relations, experimentation and 'computer optimization' as described in Detering and Etling (1985).

The TKE, can be calculated through a differential equation that equals its material derivative

$$\frac{Dk}{Dt} = \nabla \cdot \big(\frac{\nu_t}{\sigma_k}\nabla k\big) + \mathbb{P} - \epsilon \tag{2.33}$$

to an energy diffusion term, a production term and the dissipation term (Pope, 2000). σ_k is the turbulent Prandtl number and is usually equal to one so that the first term is known. The production term includes the effects of mechanical shear, for the current case,

$$\mathbb{P}_m = -\overline{v'_x v'_z}\frac{\partial v_x}{\partial z} - \overline{v'_y v'_z}\frac{\partial v_y}{\partial z} \tag{2.34}$$

and the effect of buoyancy, whose importance depends on the differences in density, that are replaced by temperature relations known from basic thermodynamics,

$$\mathbb{P}_h = \frac{g}{\theta_r}\overline{v'_z \theta'}\,, \tag{2.35}$$

where θ_r is a reference temperature (Stull, 1988). This term is well defined, therefore the only unknown is the dissipation ϵ.

The last remaining unknown requires yet another differential equation, this one of a much more empirical nature (Pope, 2000),

$$\frac{D\epsilon}{Dt} = \nabla \cdot \big(\frac{\nu_t}{\sigma_\epsilon}\nabla \epsilon\big) + C_{\epsilon 1}\,\mathbb{P}\frac{\epsilon}{k} - C_{\epsilon 2}\frac{\epsilon^2}{k}\,, \tag{2.36}$$

where the constants vary depending on the authors and flow conditions.

For this case it may be advantageous to divide the production term in two parts with different constants for the buoyancy and shear components as described in Stull (1988)

$$\frac{\partial \epsilon}{\partial t} = -\frac{\partial}{\partial z}\big(\frac{\nu_t}{\sigma_\epsilon}\frac{\partial \epsilon}{\partial z}\big) + C_{\epsilon 1 m}\frac{\epsilon}{k}\mathbb{P}_m + C_{\epsilon 1 h}\frac{\epsilon}{k}\mathbb{P}_h - C_{\epsilon 2}\frac{\epsilon^2}{k} \tag{2.37}$$

in a simplified form adapted to the current case.

Table 2.1: Parameterization constants according to several authors.

Author	$C_{\epsilon 1m}$	$C_{\epsilon 1h}$	$C_{\epsilon 2}$	σ_ϵ	σ_k	c_k
Kitada (1987)	1.44	1.44 (0 if stable)	1.92	1.3	1.0	0.09
Beljaars *et al.* (1987)	1.44	0	1.92	1.85	1.0	0.032
Duynkereke (1988)	1.46	1.46 (0 if stable)	1.83	2.38	1.0	0.033
Detering and Etling (1985)	$48.21\frac{\lvert f\rvert}{u_*}\frac{k^{3/2}}{\epsilon}$	0	1.9	1.30	0.74	0.026
Freedman and Jacobson (2002)	1.06 to 1.44	0	1.92	1.1	0.6	0.028 to 0.09

Note: u_* is the friction velocity and is defined in Section 2.4.1.

Values for all these constants have been given by several authors and there appears to be, as of yet, no indication of a certain model that would give good results for any situation.

In 1987 Kitada successfully used the model suggested by Rodi (1984) to simulate the sea breeze in a coastal region in two dimensions. He only took the production term $\mathbb{P}_h$ associated with buoyancy if the term was positive, which means that in case of a stable ABL it would have no effect. Only if it was responsible for the production of the dissipation of TKE would it be accounted for. The values for the constants used by Kitada (1987) are summarized in Table 2.1 alongside other authors.

On the same year Beljaars *et al.* (1987) presented a three dimensional model for rough terrain based on several sources. This article took into account that the atmosphere is quite different from the common cases of mechanical engineering to which the k-ϵ model is usually applied and so used a value of c_k different from the standard model. The value of $C_{\epsilon 2}$ can be measured from the decay of isotropic turbulence and is therefore very similar for all authors. The article then used a relation from the original model from Jones and Launder (1972), where

$$C_{\epsilon 2} - C_{\epsilon 1} = \frac{\kappa^2}{c_k \cdot \sigma_\epsilon} \tag{2.38}$$

and by setting the value for σ_k equal to one - meaning that the turbulent energy and the momentum have the same viscosity - and the value of $C_{\epsilon 1}$ equal to the one found elsewhere (Pope, 2000) for typical applications of mechanical engineering, Beljaars *et al.* arrived at the presented constants. It is important to notice that this article analyzed the neutrally stratified ABL only and therefore paid no attention to the buoyancy term.

A one dimensional model was presented on another journal on the same year by Duynkereke (1988). This author also used a different value for c_k close to the one employed by Beljaars *et al.* (1987) whereas $C_{\epsilon 2}$ strays slightly from the two previously mentioned authors. This is probably due to acceptable discrepancies in its measurement. As for $C_{\epsilon 1}$ a different value was chosen and making use of the same relation as Beljaars *et al.* (1987) the value of σ_ϵ is consequently also different. Much like Kitada (1987) this author also set the buoyancy term equal to zero in case it was negative.

Before any of these articles had been published Detering and Etling (1985) suggested an alteration to the TKE dissipation equation. They altered the production term by including the Coriolis effect in a characteristic length. This alteration can be seen as a mere change of the $C_{\epsilon 1}$ constant that is dependent on several variables. Their model yielded good results while keeping the other constants similar to the ones used for the standard models. It may be argued that this suggestion is arbitrary, however like many

other parameterizations these will always be simplifications of a much too complex problem like the TKE diffusion equation itself.

More recently Freedman and Jacobson (2002) made an extensive study of all the constants used in the k and ϵ equations. They based their findings on a theoretical analysis through which a range of physically acceptable values was found and then by fine tuning the parameters to a DNS simulation with conditions from the CASES 99 measurements. Their objective was to obtain a set of constants that would not lead to an ever increasing viscosity with height in the neutral case as regularly happened to the previously mentioned authors. There is no certainty regarding the value of c_k but once set $c_{\epsilon 1}$ is derived from equation (2.38).

2.3.2 k-ℓ model

When applied to the atmosphere the previous model often leads to results that are not in agreement with observations. One reason for this is because the TKE dissipation is not strong enough away from the ground which leads to a high TKE and an error in the calculation of the diffusion ν_t (Freedman and Jacobson, 2002).

Although several attempts have been made towards altering certain parameters or whole terms of the ϵ equation (Xu and Taylor, 1997) the accuracy of the previous model still has room for improvement.

Instead of using a differential equation for the TKE dissipation an algebraic equation based on experimental data can be used to determine the turbulent length scale ℓ. This quantity can be seen as the mean path traversed by a particle of air affected by a fluctuation. Being so, the difference between the horizontal velocity of an upwards moved particle and its surroundings is $\ell\,\partial v_i/\partial z$. If it is assumed that the fluctuations are approximately equal in all directions, then the averaged product of two fluctuations is $\overline{v_z' v_i'} = -\ell\,\partial|\vec{v}|/\partial z\,\ell\,\partial v_i/\partial z$ (Arya, 2001). This expression, when compared with Newton's viscosity law, leads to a turbulent viscosity equal to

$$\nu_t = \ell^2 \frac{\partial|\vec{v}|}{\partial z}\,. \tag{2.39}$$

Thus the model is closed except for an algebraic function defining the mixing length ℓ. Blackadar (1962) used experimental data from the atmosphere to deduce the following expression,

$$\ell = \frac{\kappa z}{1 + \frac{\kappa z}{\lambda}}\,, \tag{2.40}$$

that is still widely used today for its accuracy (Xu and Taylor, 1997). The constant λ is the maximum mixing length and can be determined as $2.7 \times 10^{-4}\,|\vec{G}|/|f|$ (Blackadar, 1962) or as $6.3 \times 10^{-3}\,u_*/|f|$ (Blackadar, 1965) with u_* being the friction velocity. While the second was an improvement on the first, the first version has seen a wider application.

However, the accuracy of the model can be further increased if the TKE equation is added. The equation for the turbulent viscosity can be seen as the product of a characteristic length, in this case the mixing length, and a characteristic velocity u_ℓ, in this case $\ell\,\partial|\vec{v}|/\partial z$. If so then some assumptions can be made regarding this last quantity. By using the tubulent velocity scale defined as the square root of the TKE (Arya, 2001) and assuming that u_ℓ is related to the turbulent velocity scale in a linear manner, it can

be shown (Detering and Etling, 1985) that the proportionality constant is equal to $c_k^{1/4}$, so that

$$\nu_t = \ell \, c_k^{1/4} k^{1/2} \, . \tag{2.41}$$

From this one and equation (2.32) the relation for the TKE dissipation,

$$\epsilon = \frac{c_k^{3/4} \, k^{3/2}}{\ell} \tag{2.42}$$

can be deduced thereby closing the differential equation for the TKE. It is debatable whether the length scale for the TKE diffusion is in fact the same as for the turbulent viscosity (Weng and Taylor, 2003). This is the formulation for the one equation k-ℓ model for which, unlike in the previous model, only one differential equation has to be solved in order to obtain the turbulent viscosity. Some models do not rely solely on ℓ or on ϵ but make use of the two simultaneously, thus exploiting the adaptability of the first model and the accuracy of the second model.

2.4 Stability

2.4.1 Surface Layer

Due to its accessibility and relevance for human activities the lowest part of the atmosphere, the surface layer (SL), has received significant interest from the geophysical and engineering communities. Data for this region is more abundant which allowed for several parameterizations. These are especially important for turbulence models like the k-ϵ, since one of its weak points is precisely the prediction of quantities near the walls which may in turn spread inaccuracies to the center of the domain.

A well known relation for the behaviour of a flow near a wall is given by the logarithmic profile law, which can be deduced from similarity theory assuming that the momentum flux is constant in this region. If so the only relevant quantities are the friction velocity, $u_* = \sqrt{\tau_0/\rho}$, and the height z, being τ_0 the shear stress close to the wall. Under these conditions, the velocity gradient is given by (Arya, 2001)

$$\frac{z}{u_*} \frac{\partial |\vec{v}|}{\partial z} = \frac{1}{\kappa} \, , \tag{2.43}$$

where κ is a constant obtained from experimental data and that is given a value of 0.4 in this work as by most authors in the past few years; *e.g.* Detering and Etling (1985), Apsley and Castro (1997) or Freedman and Jacobson (2002).

This expression however is not enough to describe the stable or unstable surface layer since the heat flux leads to differences in the wind speed profile.

In order to account for this the Monin-Obukhov similarity theory (MOST) introduces two new variables. The kinematic heat flux $\overline{v_z' \theta'}_0$ and a buoyancy variable g/θ_0 where θ_0 is a reference temperature for the SL. With the assumption that these four variables are enough to define the phenomena in the SL a stability parameter,

$$\zeta = \frac{z}{\mathcal{L}}, \tag{2.44}$$

is deduced where the characteristic Obukhov length is given by (Arya, 2001)

$$\mathcal{L} = \frac{u_*^2\,\theta_0}{\kappa\, g\,\theta_*}\,. \tag{2.45}$$

From these parameters a correction to the logarithmic profile law can be deduced for both the temperature and velocity gradients. A general formulation adopted by Dyer (1974) describes several models,

$$\phi_m(\zeta) = \frac{\kappa\, z}{u_*}\frac{\partial|\overline{v}|}{\partial z} = \begin{cases} (1-\beta_{mu}\,\zeta)^{-\frac{1}{4}}\,, & \text{for } \zeta < 0, \\ 1+\beta_{ms}\,\zeta\,, & \text{for } \zeta \geq 0, \end{cases} \tag{2.46}$$

$$\phi_h(\zeta) = \frac{\kappa\, z}{\mathrm{Pr}_n\,\theta_*}\frac{\partial\theta}{\partial z} = \begin{cases} (1-\beta_{hu}\,\zeta)^{-\frac{1}{2}}\,, & \text{for } \zeta < 0, \\ 1+\dfrac{\beta_{hs}}{\mathrm{Pr}_n}\,\zeta\,, & \text{for } \zeta \geq 0, \end{cases} \tag{2.47}$$

where the newly introduced ϕ_m and ϕ_h are obtained from fittings to experimental data and thus have different β constants depending on the author.

The solution given by Högström (1988) will be used in all parmameterizations for the SL so that

$$\beta_{mu} = 19.3\,; \qquad \beta_{hu} = 11.6\,; \qquad \beta_{ms} = 4.8\,; \qquad \beta_{hs} = 8\,; \qquad \mathrm{Pr}_n = 0.95\,. \tag{2.48}$$

In order to obtain the wind speed and temperatures in the surface layer the previous equations have to be integrated to give

$$|\vec{v}| = \frac{u_*}{\kappa}\left[\ln\!\left(\frac{z}{z_{m0}}\right) - \psi_m(\zeta) + \psi_m\!\left(\frac{z_{m0}}{z}\,\zeta\right)\right], \tag{2.49}$$

$$\Delta\theta = \frac{\mathrm{Pr}_n\,\theta_*}{\kappa}\left[\ln\!\left(\frac{z}{z_{h0}}\right) - \psi_h(\zeta) + \psi_h\!\left(\frac{z_{h0}}{z}\,\zeta\right)\right], \tag{2.50}$$

as described in Veiga Rodrigues *et al.* (2016). The integration constants z_{m0} and z_{h0} can be obtained from measurements to the SL, being then representative of the surface roughness height. The functions ψ_m and ψ_h result from the integration of the $\phi_{m,h}$ functions so that

$$\psi_m(\zeta) = \begin{cases} \ln\!\left(\dfrac{[1+\eta^2][1+\eta]^2}{8}\right) - 2\,\mathrm{atan}\,(\eta) + \dfrac{\pi}{2}, & \text{for } \zeta < 0, \\ -\beta_{ms}\,\zeta, & \text{for } \zeta \geq 0, \end{cases} \tag{2.51}$$

$$\psi_h(\zeta) = \begin{cases} 2\,\ln\!\left(\dfrac{1+\chi}{2}\right), & \text{for } \zeta < 0, \\ -\dfrac{\beta_{hs}}{\mathrm{Pr}_n}\,\zeta\,, & \text{for } \zeta \geq 0, \end{cases} \tag{2.52}$$

with $\eta = (1-\beta_{mu}\,\zeta)^{\frac{1}{4}}$ and $\chi = (1-\beta_{hu}\,\zeta)^{\frac{1}{2}}$. From (2.49) and (2.50) the surface-layer dimensionless variables for momentum and heat, u^+ and θ^+, are defined as

$$u^+ = \frac{|\vec{v}|}{u_*} = \frac{1}{\kappa}\left[\ln\!\left(\frac{z}{z_{m0}}\right) - \psi_m(\zeta) + \psi_m\!\left(\frac{z_{m0}}{z}\,\zeta\right)\right], \tag{2.53}$$

$$\theta^+ = \frac{\Delta\theta}{\theta_*} = \frac{\mathrm{Pr}_n}{\kappa}\left[\ln\!\left(\frac{z}{z_{h0}}\right) - \psi_h(\zeta) + \psi_h\!\left(\frac{z_{h0}}{z}\,\zeta\right)\right]. \tag{2.54}$$

Other parameterizations or sets of constants for the surface layer exist; *e.g.* Dyer (1974) or Högström (1988).

2.4.2 Atmospheric Boundary Layer

In the bulk of the ABL the SL relationships have no real meaning and therefore another parameter for stability is required. A relation between buoyancy forces, represented by the Brunt-Väisälä frequency $N = \sqrt{g/\theta\,\partial\theta/\partial z}$, and shear, represented by the velocity gradient, is given by the Richardson number defined as (Arya, 2001)

$$\mathrm{Ri} = \frac{N^2}{|\partial\vec{v}/\partial z|^2} = \frac{g}{\theta_r}\frac{\partial\theta}{\partial z}\left|\frac{\partial\vec{v}}{\partial z}\right|^{-2}, \tag{2.55}$$

where the potential temperature in the denominator is approximated by the reference potential temperature. This is a valid assumption if it is chosen appropriately so as not to differ too greatly from the temperatures in the atmosphere.

If the Brunt-Väisälä frequency is very high when compared to the velocity gradient this means that the destruction of TKE due to the buoyancy term is also high compared to its production caused by mechanical shear. In this case the turbulence will eventually be suppressed which would lead to a nonexistent turbulent viscosity. In cases like this a state of intermittent turbulence can be observed in the atmosphere and the turbulent viscosity is no longer correctly described by equation (2.32). This only happens for strong stratification when the Richardson number approaches its critical value somewhere between 0.2 to 0.5 (Arya, 2001).

Another parameter of interest is the relation between TKE buoyant and mechanical production terms. The flux Richardson number is defined as

$$\mathrm{Rf} = \frac{-\mathbb{P}_h}{\mathbb{P}_m} = \frac{N^2}{\mathrm{P}_r\,|\partial\vec{v}/\partial z|^2}\,. \tag{2.56}$$

Chapter 3

Computational Implementation

Since no analytic solution is known for the set of equations previously presented describing turbulent and averaged quantities, a discretization of the differential formulation is needed so that it may afterwards be solved by a computer. Because the geometry of the problem is very simple the Finite Difference method was chosen which allows for an easy and effective implementation. Due to the particular formulation used the conservation equation is ensured.

A solution for a general transport equation will be explained and the particular solutions for the momentum, temperature, k and ϵ will be presented afterwards. It will be obvious that these can all be treated similarly.

A general transport equation

$$\frac{\partial \phi}{\partial t} = \frac{\partial}{\partial z}\left(\Gamma \frac{\partial \phi}{\partial z}\right) + S \tag{3.1}$$

will be used as example to briefly describe the numerical techniques employed in this work. In it, ϕ is the field variable being solved, Γ is the diffusion coefficient and S is a term used to represent any source, sink, momentum, body force or any similar quantity.

3.1 Meshing

The domain is first divided into several cells in whose center the values of all relevant properties are stored to be used for calculations. Since all gradients are generally strongest near the wall a tighter mesh is used in this region which becomes gradually wider with increasing height. A geometric progression was used to define the cell heights. By using a common mesh factor f_m, an arbitrary cell will have $(z_{ti} - z_{bi}) = (z_{t0} - z_{b0})\, f_m^i$, where i is the node index and t or b represent the top or bottom face. Using the Newton-Raphson method a value for f_m is calculated that satisfies the conditions of the bottom cell height and total domain height. For the total height the Obukhov length can be used as a reference so as to guarantee sufficient room for the development of the whole profile. After analyzing several results a total of 50 nodes where chosen as the best compromise between computation time and accuracy for all simulations unless stated otherwise. The reasons for this choice are explained in Appendix A.

3.2 First Spatial Derivative

The first derivative appears in the production terms of the TKE and its dissipation, the diffusion terms will get a different approach from the one subsequently described. A three point interpolation is used to approximate a given quantity, ϕ, as a continuous polynomial. Since the polynomial has an analytic derivative the problem is solved. The derivative in a certain node is thus a function of the node itself and the ones directly next to it. If the polynomial used is the simple Lagrange polynomial for a three point interpolation its derivative can be written as

$$\frac{\partial \phi}{\partial z} = \phi_B \frac{2z - z_T - z_P}{(z_B - z_T)(z_B - z_P)} + \phi_P \frac{2z - z_T - z_B}{(z_P - z_T)(z_P - z_B)} + \phi_T \frac{2z - z_P - z_B}{(z_T - z_P)(z_T - z_B)} \tag{3.2}$$

where T, B and P stand for the top, bottom and central nodes respectively. For the current case the derivatives will be evaluated at the nodes. In order to simplify the implementation three vectors $dzct$, $dzcb$ and $dzcp$ are defined such that

$$\frac{\partial \phi}{\partial z}_P = \phi_B \, dzcb + \phi_P \, dzcp + \phi_T \, dzct. \tag{3.3}$$

3.3 Time Derivative

Since the material derivatives are entirely reduced to their time derivative the calculation for the node in question depends only on itself and not on any neighboring nodes. However the previous instants will be relevant. For this case a simple second order discretization was used that employs the two previous instants with indexes $j-1$ and $j-2$ for one and two time steps before the current time j. The time steps, Δt, are fixed so that (Perić and Ferziger, 2002)

$$\frac{\partial \phi}{\partial t} = \frac{3\,\phi^j - 4\,\phi^{j-1} + \phi^{j-2}}{2\,\Delta t}\,. \tag{3.4}$$

This scheme can be made implicit,

$$\frac{\partial \phi}{\partial t} = f(\phi(t)) \Rightarrow 3\,\phi^j - 4\,\phi^{j-1} + \phi^{j-2} = 2\,\Delta t\, f(\phi^j)\,, \tag{3.5}$$

thus requiring iterations to reach convergence before advancing to the next time step.

3.4 Diffusive Term

This term was treated with an approach that is similar to the finite-volume method where the values of diffusivity and gradient are to be calculated at the cell faces through interpolation and in this particular case a simple first order method was used for Γ where

$$\Gamma_t = \frac{z_t - z_P}{z_T - z_P}\Gamma_P + \frac{z_T - z_t}{z_T - z_P}\Gamma_T \tag{3.6}$$

and the value for the bottom face is the value of the top face from its bottom node. The derivatives at the faces are simply given by $\Delta\phi/\Delta z$ with the top and central nodes, in the

case of the top face and analogously for the bottom face. This can be done because the faces are precisely halfway between nodes. The same method is then used to calculate the derivative of $\Gamma \cdot \partial\phi/\partial z$ but this time with the face values so that

$$\frac{\partial}{\partial z}\left(\Gamma\frac{\partial\phi}{\partial z}\right) \Rightarrow \frac{\left(\Gamma\frac{\partial\phi}{\partial z}\right)_t - \left(\Gamma\frac{\partial\phi}{\partial z}\right)_b}{z_t - z_b}. \tag{3.7}$$

As was stated previously this is similar to the Finite Volume formulation. Integrating the diffusion over the volume of a cell and making use of the Gauss theorem

$$A_{cell}\int_{z_1}^{z_2}\frac{\partial}{\partial z}\left(\Gamma\frac{\partial\phi}{\partial z}\right)dz = A_{cell}\left[\left(\Gamma\frac{\partial\phi}{\partial z}\right)_t - \left(\Gamma\frac{\partial\phi}{\partial z}\right)_b\right] \tag{3.8}$$

and then dividing by the volume of the cell equation (3.7) is obtained.

3.5 Solver

In order to solve the transport equations for each node a matrix **A** is built such that, when multiplied with the vector of the quantity in question, it will result in a source vector $\vec{b}$. The matrix will thus contain all the coefficients that are to be multiplied with ϕ, but since only first derivatives or diffusive terms are present across all equations only the values of the neighboring nodes and the central node itself are required, which results in a banded matrix with a top ($\vec{a_T}$), bottom ($\vec{a_B}$) and central ($\vec{a_P}$) diagonal. The coefficient of ϕ_P from its time derivative will also be added to the central band of the matrix. The source vector will contain all explicit terms. These may depend on the values of ϕ from a previous iteration but will tend to a fixed value on convergence. Undoubtedly the upper and lower bands have a smaller size than the central one due to the corners. This can be solved by adding the excess coefficients to the central band as

$$\begin{bmatrix} a_{B1}+a_{P1} & a_{T1} & 0 & 0 & \dots \\ a_{B2} & a_{P2} & a_{T2} & 0 & \dots \\ \ddots & \ddots & \ddots & \ddots & \ddots \\ \dots & 0 & a_{B(n-2)} & a_{P(n-2)} & a_{T(n-2)} \\ \dots & 0 & 0 & a_{B(n-1)} & a_{P(n-1)}+a_{T(n-1)} \end{bmatrix} \cdot \begin{bmatrix} \phi_1 \\ \phi_2 \\ \vdots \\ \phi_{n-2} \\ \phi_{n-1} \end{bmatrix} = \begin{bmatrix} b_1 \\ b_2 \\ \vdots \\ b_{n-2} \\ b_{n-1} \end{bmatrix}, \tag{3.9}$$

which is in accordance with a zero gradient at the boundaries. This is the Neumann boundary condition (Perić and Ferziger, 2002) and will be imposed if no other is present. In order to solve this equation system an optimized solver for banded matrices was used. When creating the matrices it is preferable to have a diagonally dominant one where the central band has a higher value than the sum of all other coefficients on that same line. This ensures that the matrix will converge (Perić and Ferziger, 2002).

Another typical boundary condition, the Dirichlet condition, prescribes ϕ at the top and bottom boundaries by sending the top coefficient of the last line to the source term multiplied by its corresponding quantity ϕ_n and vice-versa for the first line so that

$$\begin{bmatrix} a_{P1} & a_{T1} & 0 & 0 & \dots \\ a_{B2} & a_{P2} & a_{T2} & 0 & \dots \\ \ddots & \ddots & \ddots & \ddots & \ddots \\ \dots & 0 & a_{B(n-2)} & a_{P(n-2)} & a_{T(n-2)} \\ \dots & 0 & 0 & a_{B(n-1)} & a_{P(n-1)} \end{bmatrix} \cdot \begin{bmatrix} \phi_1 \\ \phi_2 \\ \vdots \\ \phi_{n-2} \\ \phi_{n-1} \end{bmatrix} = \begin{bmatrix} b_1 - a_{B1}\phi_0 \\ b_2 \\ \vdots \\ b_{n-2} \\ b_{n-1} - a_{T(n-1)}\phi_n \end{bmatrix}, \tag{3.10}$$

which makes it useful for guaranteeing a geostrophic velocity at the top node for example.

3.6 Momentum

The momentum equations (2.25), (2.26) can be rewritten as

$$\frac{\partial v_x}{\partial t} = f\left(v_y - G_y\right) + \frac{\partial}{\partial z}\left(\left(\nu_t + \nu_{mol}\right)\frac{\partial v_x}{\partial z}\right), \tag{3.11}$$

$$\frac{\partial v_y}{\partial t} = -f\left(v_x - G_x\right) + \frac{\partial}{\partial z}\left(\left(\nu_t + \nu_{mol}\right)\frac{\partial v_y}{\partial z}\right), \tag{3.12}$$

where the first term on the right-hand side of the equations represents the difference between the Coriolis and pressure force, whose treatment was made explicit. The source vector $\vec{b}$ will also include the past velocities from the time derivative. While the x and y equations are solved separately, with this formulation the matrix $\mathbf{A}$ is the same for x and y components of velocity, thus only one matrix is required. On the other hand the source term requires different vectors for each due to the different components of the geostrophic wind speed and the direction of the Coriolis force. Although the molecular viscosity is not relevant when compared to the turbulent one it is still preserved in the equations for numerical stability.

The top boundary is treated with a simple Dirichlet condition where the geostrophic wind speed is enforced. The bottom node has a prescribed shear stress on its lower face given by relations from the surface layer so that its momentum equation in x becomes

$$\frac{\partial v_x}{\partial t} - f\left(v_y - G_y\right) = \frac{\left(\nu_t \frac{\partial v_x}{\partial z}\right)_t - {u_*}^2}{z_t - z_b} \tag{3.13}$$

and similarly in the other direction. With this condition the velocity at the boundary node is no longer present so that the corresponding matrix coefficients are set to zero. The velocity is known *a priori* to vanish at the surface so this value can be imposed after the solver is applied. Using this sort of formulation increases accuracy since the velocity profile is logarithmic and therefore its shear stress is better described by surface layer relationships, ${u_*}^2$, than the discretized gradient multiplied by the turbulent viscosity, $\left(\nu_t \frac{\partial v_x}{\partial z}\right)_b$.

3.7 Turbulent Kinetic Energy

The previous section regarding the momentum equation still requires that the turbulent viscosity be calculated, which, making use of the k-ϵ relations, requires the TKE. From equation (2.33)

$$\frac{\partial k}{\partial t} = \frac{\partial}{\partial z}\left(\left(\frac{\nu_t}{\sigma_k} + \nu_{mol}\right)\frac{\partial k}{\partial z}\right) + \nu_t\left(\left(\frac{\partial v_x}{\partial z}\right)^2 + \left(\frac{\partial v_y}{\partial z}\right)^2\right) - \frac{\nu_t}{\mathrm{Pr}}\frac{\partial \theta}{\partial z}\frac{g}{\theta_0} - \epsilon\,, \tag{3.14}$$

that gets a very similar treatment to the momentum equation system for the first and second terms. The third and fourth related to mechanical and buoyancy production respectively are totally explicit requiring the velocity and temperature at each node. The TKE dissipation, on the other hand, is treated implicitly thus increasing $\vec{a_p}$ which is beneficial for the solver. In order to achieve this the TKE diffusion is calculated locally from the previous TKE and turbulent viscosity according to equation (2.32).

In order to avoid the complete destruction of TKE by the buoyancy term and knowing that the critical Richardson is no smaller than 0.2 the buoyancy term is limited to 20% of the shear production whenever the conditions are of local stability.

For the lower boundary the constant flux assumption valid for the SL is made, thus the null gradient condition is enforced. The top is treated with a Dirichlet boundary condition in the solver after which the last node is equaled to the penultimate.

3.8 TKE dissipation

Making use of the already calculated and unchanged values of the mechanical and buoyant production of TKE there is no need to recalculate them for the dissipation. Recalling equation (2.36)

$$\frac{\partial \epsilon}{\partial t} = -\frac{\partial}{\partial z}\left(\frac{\nu_t}{\sigma_\epsilon}\frac{\partial \epsilon}{\partial z}\right) + C_{\epsilon 1 m}\frac{\epsilon}{k}\mathbb{P}_m + C_{\epsilon 1 h}\frac{\epsilon}{k}\mathbb{P}_h - C_{\epsilon 2}\frac{\epsilon^2}{k}\,, \tag{3.15}$$

the Production terms can be treated either explicitly by using ϵ from the previous iteration or implicitly, however the implicit formulation could lead to a less stable matrix *i.e.* depending on their sign, since these terms would have to be subtracted from the main diagonal, it could cease to be diagonally dominant and promote divergence. The explicit formulation was therefore chosen whenever possible, however, instead of using the lastly calculated value of TKE diffusion the ratio ϵ/k is estimated from the newest values of viscosity and TKE making use of (2.32) so that the production of TKE dissipation becomes

$$C_{\epsilon 1}\frac{c_k k}{\nu_t}\mathbb{P}\,. \tag{3.16}$$

As for the quadratic term, representing the dissipation of the TKE dissipation, a fully explicit or partially implicit formulation can be used. In the first case the coefficient would be multiplied with the solution of the previous iteration and added to the source term while simultaneously being subtracted from the matrix. In the second case, since this term is negative, it will be added to the main diagonal so that the half implicit formulation was chosen with a similar formulation to the one used for the production term using the k-ϵ relation in equation (2.32), where ϵ is the one from the present iteration,

$$-C_{\epsilon 2}\frac{c_k k}{\nu_t}\epsilon\,. \tag{3.17}$$

Having defined the system of equations for the core of the matrix, the boundary conditions are then applied. For the bottom a simple prescription of the TKE dissipation is used from the surface layer relationships as Duynkereke (1988)

$$\epsilon = \frac{{u_*}^3}{\kappa z}\left[\phi_m - \frac{z}{\mathcal{L}}\right] \tag{3.18}$$

applied to the first node above the ground. The zeroth node is not relevant in this case since, as will be shown later, the viscosity for the first and second nodes are prescribed with relations different from the one for k-ϵ used for the core, equation (2.32). Thus there is no real use for the TKE dissipation at ground level, whose physical meaning would be questionable in any case. As for the top of the domain a simple Dirichlet boundary condition is used. After solving the matrix the last node is then equaled to the penultimate one so as to ensure a zero gradient just like Weng and Taylor (2003).

3.9 Viscosity

Making use of the SL relations the lower boundary and the bottom node are treated with

$$\nu_t = \frac{u_* \ \kappa z}{\phi_m} \tag{3.19}$$

The value thus obtained for the first node then sets the lower limit for all other nodes.

3.10 Temperature

By substituting the second order momentum given by the the turbulence model into the temperature equation (2.18) one obtains

$$\frac{\partial \theta}{\partial t} = \frac{\partial}{\partial z}\left[\left(\frac{\nu_t}{\mathrm{Pr}} + \alpha \right) \frac{\partial \theta}{\partial z} \right] \tag{3.20}$$

where α, the thermal diffusivity, is inserted for numerical stability playing a role similar to the molecular viscosity in the momentum equation. The potential temperature is then separated into a fixed reference θ_0 and a perturbation temperature $\hat{\theta}$ with the first becoming a source term.

$$\frac{\partial \hat{\theta}}{\partial t} = \frac{\partial}{\partial z}\left[\left(\frac{\nu_t}{\mathrm{Pr}} + \alpha \right) \frac{\partial \theta_0}{\partial z} \right] + \frac{\partial}{\partial z}\left[\left(\frac{\nu_t}{\mathrm{Pr}} + \alpha \right) \frac{\partial \hat{\theta}}{\partial z} \right] \tag{3.21}$$

The diffusion for both the reference temperature and the perturbation temperature are calculated as in the previous cases.

Similarly to the momentum equation the lower boundary is treated by prescribing the heat flux on its bottom face as $\theta_* u_*$. Assuming a constant flux surface layer and employing the stability functions

$$\frac{\left[(\nu_t + \alpha) \frac{\partial \theta}{\partial z} \right]_t - u_* \theta_*}{z_t - z_b} \tag{3.22}$$

is used for the lower boundary diffusion. The upper node is treated with a Dirichlet condition in the solver. The temperature at the upper boundary is then extrapolated from the last and penultimate nodes at the end of every iteration.

Chapter 4

Simulation of the Neutrally-Stratified ABL

In the following chapter five models for the neutrally stratified ABL will be presented and their results will be shown for simulations under two sets of conditions. The first is under a neutrally stratified atmosphere for which the steady-state was achieved, the second analyses its evolution over a period of 32 *h.*

4.1 Steady State

In 1931 an experiment undertaken by Mildner (1932) consisted in the measurement of the velocities of 28 meteorological balloons launched in an airfield near Leipzig. The original data was analyzed and reprinted in Lettau (1950). The area was plain and grass-covered, a potential temperature lapse rate of 3.5°C/km was measured nearby, the pressure gradient did not change with height and there were no signs of convection. It is speculated that even though the wind came from the city nearby, its effect on turbulence was negligible. Obviously these conditions are not those of a neutrally stratified ABL, however the measurements have served as a reference for several authors wanting to compare or tune models with reality (*e.g.* Detering and Etling (1985); Duynkereke (1988)). This is because a truly neutrally stratified ABL is an idealized case that rarely takes place in the real atmosphere for a sufficiently long period of time to deem it as a steady-state flow.

Lettau (1950) also presented values for the surface shear stress, geostrophic wind speed, 17.51 m/s, and the Coriolis parameter, 1.4×10^{-4} s^{-1}. From these and making use of SL relations the friction velocity could be calculated as 0.65 m/s, which is a value that was used by several authors (*e.g.* Detering and Etling (1985), Apsley and Castro (1997)). The roughness length was presented by Detering and Etling (1985) as being of 0.3 m. It is debatable whether this vale is accurate or not, since according to the description of Lettau (1950) regarding the experiment the ground was an airfield near the city of Leipzig with little vegetation. According to a diagram from the Royal Aeronautical Society (1973) printed in Arya (2001) the roughness height for such a region should be around 0.01 m. Furthermore by applying the logarithmic profile law to the first measurement at a height of 50 m the roughness height can be estimated at 0.01 m. Whether this height is beyond the surface layer where the logarithmic profile law is no longer valid is uncertain.

The Rossby-number similarity theory valid for a neutral ABL states that the characteristic height $h = u_*/|f|$ is proportional to the ABL depth. It can then be shown that the Rossby number, $\mathrm{Ro} = |\vec{G}||f|/z_0$, guarantees, within the assumptions made for this simplification, similarity between different cases (Arya, 2001).

Simulations for several values of Rossby number imply that the value of 0.3 m proposed by Detering and Etling (1985) is indeed correct since it fits the measured profiles better. Possible reasons for this discrepancy between calculated and employed values for the roughness height can be due to an error-inducing description of the surface type by Lettau (1950) or an unlucky data-set that suggests certain values of z_0 because the profile was not fully developed. Another possibility is because the models do in fact simulate a roughness height of 0.01 m better if fed with a value of 0.3 m instead for this particular case, suggesting that they are not entirely reliable for the whole range of Rossby numbers.

4.1.1 Description of the ABL Models

k-ϵD

The k-ϵD model used the k-ϵ equations with the constants as defined in Table 2.1 according to Duynkereke (1988) . In order to match the Leipzig wind profile it was run until it achieved a steady state and the differences between solutions for consecutive iterations were minimal. The roughness height was set to 0.3 m as in Detering and Etling (1985) and likewise the geostrophic wind speed equal to 17.51 m/s in the x direction while $G_y = 0$ m/s. Since the case is neutrally stratified (no heat flux or temperature gradient) the Obukhov length is infinite. For the same reason the temperature equation was not used. In order to determine the computational domain height the Rossby similarity was used. The height of the neutral ABL is about $0.25\,u_*/f$ (Arya, 2001). However since for this model in particular there is a clear relation between the solution and the domain height the latter was set to three times u_*/f.

k-ϵF

The k-ϵF model is an attempt to correct k-ϵD by doing a simple adjustment to its parameters, specifically the TKE dissipation equation constants. The conditions are exactly the same as for k-ϵD. The constants used are the ones presented by Freedman and Jacobson (2002). They did not specify the value of c_k but different values from the one used in k-ϵD led to no clear improvement of the results. Although a value of 0.09 did reduce the boundary-layer height it also led to a greater deviation between the measured and calculated friction velocities. Thus a value of 0.033 was chosen for c_k which results in $C_{\epsilon 1} = 1.12$ according to equation (2.38), whereas the remaining constants are as defined in Table 2.1.

ℓB

The ℓB model is simply an application of the algebraic expression derived by Blackadar (1965) regarding the mixing length. Unlike all other models there is no prognostic equation for the TKE. Thus the mixing length is calculated according to equation (2.40) and the turbulent viscosity to equation (2.39). The fact that the mixing length is given by

a relation that is strongly based on observations for the particular case of a barotropic, horizontally homogeneous atmosphere gives it a strong connection to reality, however the model is probably not able to simulate more complex situations.

Using the previously defined conditions of the Leipzig wind profile a simulation was run with a time-scheme whose role was merely of relaxing the convergence. Though the residuals of the present model were higher than for the first two models, it is considered that a steady-state has been achieved for the presented results (this assumption is validated with the analysis of the transient case). Any residuals were due to small oscillations on the upper third of the domain. A domain height of u_*/f was sufficient for all quantities to develop with height.

This model provides no results for the TKE dissipation, however these can be calculated in a post-processing phase. In order to compare results with the Leipzig wind profile the results by Blackadar (1962) were used. This author calculated the mixing length from the wind profiles and from these results the TKE dissipation could be calculated, since according to the same article $\epsilon = v_t^3/\ell^4$.

k-ℓ**B**

The k-ℓB model is based on the k-ℓ formulation described in Section 2.3.2, so that there is a prognostic equation for the TKE, equation (2.33), and an algebraic equation for the mixing length as provided by Blackadar (1965), equation (2.40). The turbulent viscosity is then calculated from these two quantities according to equation (2.41). The fact that the mixing length was obtained from direct observations of the atmosphere gives this model a stronger connection to reality than the ones using the TKE dissipation equation. However, there is no physical meaning to the diagnostic ℓ equation, though it may be argued that the TKE dissipation equation is also lacking in physical meaning. The TKE equation used the same boundary conditions as for the k-ϵ models described in section 2.3.1.

The model was run with a domain height of $0.5u_*/f$, which was enough for the profile to develop over the height of the ABL. A time-scheme was used to aid convergence. Like in ℓB a steady state was achieved. The coefficient for the viscosity equation, c_k was set to 0.033 and the outer conditions from the Leipzig wind profile of roughness height and pressure gradient were prescribed as aforementioned.

k-ϵ-ℓ**X**

The k-ϵ-ℓX model is an application of the alteration to the k-ϵ model suggested by Xu and Taylor (1997). The model differs from the standard one in the prognostic equation for ϵ, where the production term is assumed to be equal to $\mathbb{P}_\epsilon = C_{\epsilon 1} c_k^{3/4}\, k^2/\ell^2$. Thus the equation for the TKE dissipation becomes:

$$\frac{D\epsilon}{Dt} = \nabla \cdot \left(\frac{\nu_t}{\sigma_\epsilon}\nabla\epsilon\right) + C_{\epsilon 1} c_k^{3/4}\, \frac{k^2}{\ell^2} - C_{\epsilon 2}\frac{\epsilon^2}{k}\,. \tag{4.1}$$

This was an attempt to correct this equation since it was held responsible for the unsuitability of the standard model to the atmosphere by the authors. Were it not so, but if the problem lay in the TKE prognostic equation then k-ℓB would tend to yield results that were also different from observations like in the k-ϵ models. Furthermore, the fact that

the physical basis of the TKE equation is much stronger than the one of the TKE dissipation also makes alterations to the last one more desirable so as to maintain coherence. The mixing length was calculated according to Blackadar (1965).

Having ϵ the TKE is computed from equation (2.33) and ν_t afterwards from equation (2.41), similarly to the k-ℓ model. In order to avoid a zero viscosity that could lead to awkward solutions and momentary spikes in velocity (which could hinder convergence and create oscillations), a lower limiter was set forcing its value to no less than 10 times the molecular viscosity. The impact of using this limitation or the one generally applied to all models as described in Chapter 3 is not noticeable.

The model was allowed to converge reaching an almost steady-state like the previous cases and the outer conditions were the ones from the Leipzig wind profile.

4.1.2 Results

The most relevant parameters have been plotted for all models in figures 4.1, 4.2 and 4.3, except for the ℓB for which the TKE was not calculated. Rossby similarity theory was used to adimensionalize all quantities. The values of u_* and maximum wind speeds in both directions are presented in Appendix B with the respective errors.

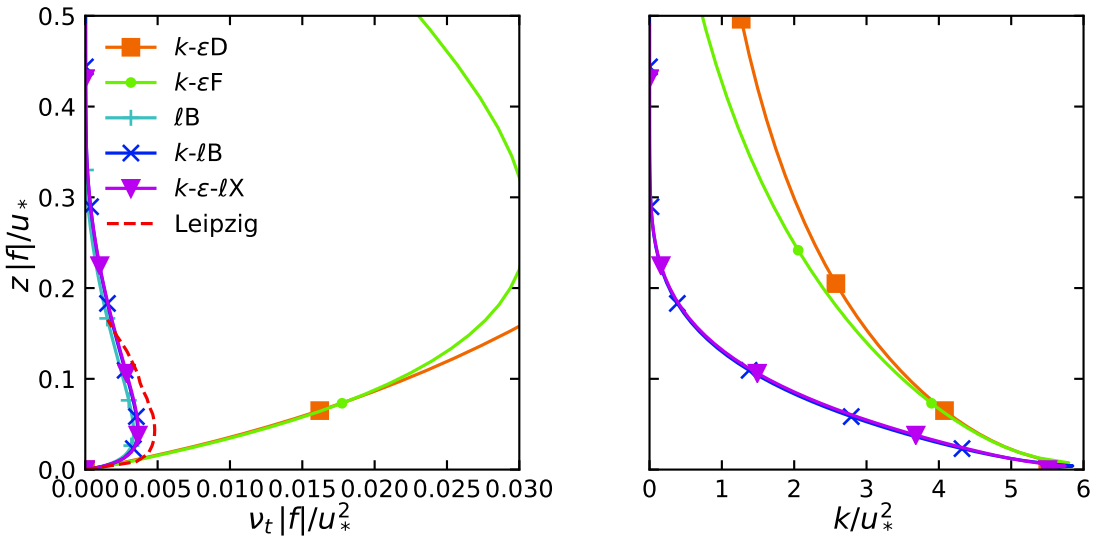

Figure 4.1: Results for the adimensionalized ν_t (left) and k (right) as a function of the adimensional height for the steady-state models and the Leipzig wind profile. The TKE from ℓB was not plotted due to its formulation.

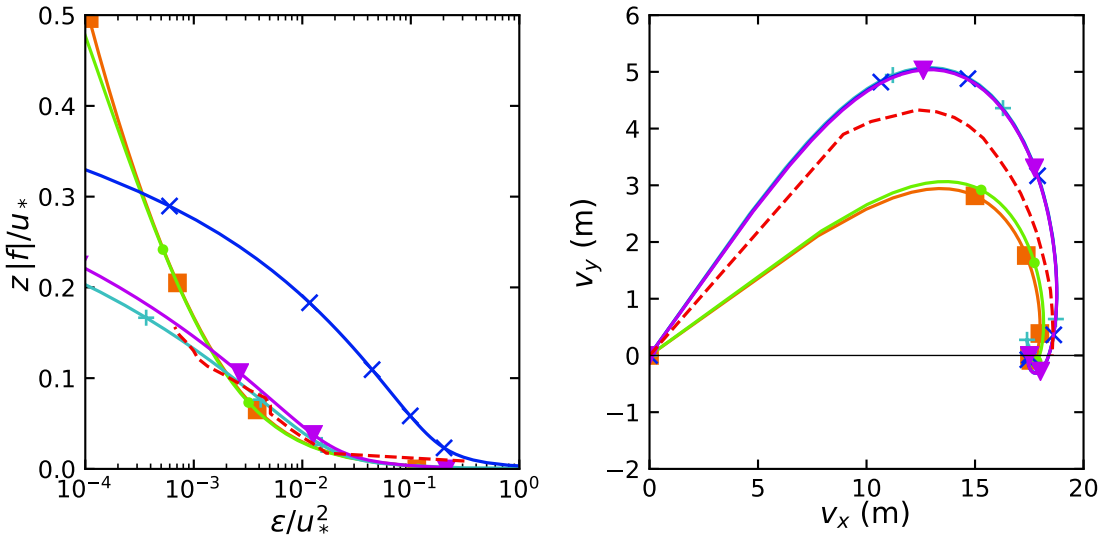

Figure 4.2: Results for the adimensionalized ϵ as a function of the adimensional height (left) and the calculated Ekman spiral (right). k-ℓB had its ϵ calculated according to equation (2.42). For further details, please refer to Figure 4.1.

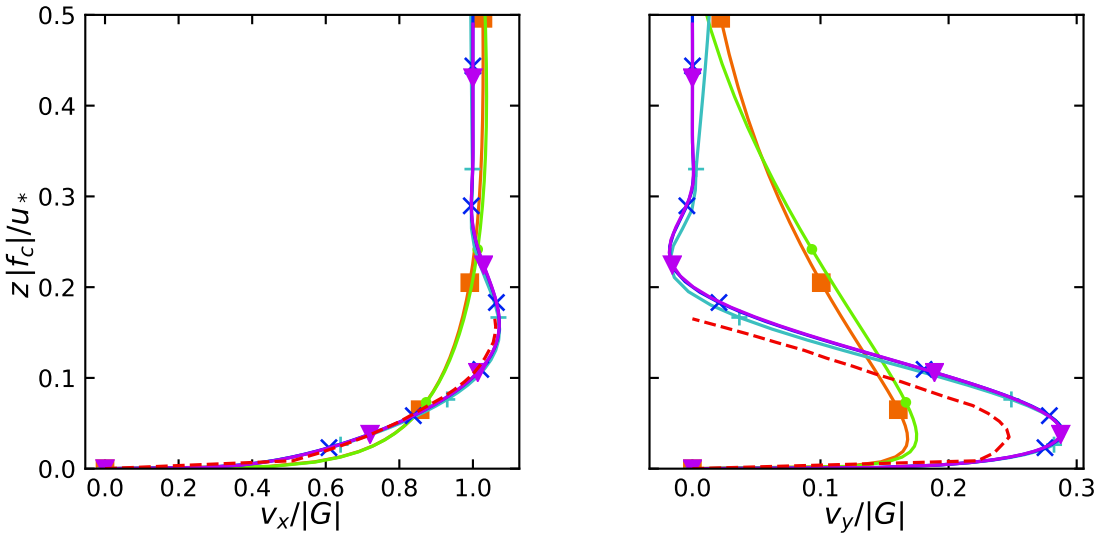

Figure 4.3: Results for v_x and v_y adimensionalized by the magnitude of the geostrophic wind as a function of the adimensional height. For further details, please refer to Figure 4.1.

4.1.3 Analysis

Although k-ϵD is meant for atmospheric flows its prediction is poor in regard to the Leipzig wind profile. The turbulent viscosity tends to grow with height in an unbounded manner, with the domain height influencing this rate. The fact that $\partial \nu_t / \partial z$ never becomes zero makes the top boundary condition imposing a zero gradient a limiting factor whose influence is diffused through the upper part of the domain. The fact that the viscosity does not have the characteristic maximum seen in the Leipzig wind profile leads to an inaccurate velocity profile whose prediction worsens with height. When near the ground however the model seems to be close to reality and may in fact be better than others for the first few meters such as flows around trees or buildings. The way the model was run is in itself an abstraction from reality since the neutral ABL is not affected by a zero lapse rate all the way to $3u_*/f$. At the ABL top there should be an increase in potential temperature that could lead to a suppression of turbulence and eventually of the turbulent viscosity. If run with a lower top the model leads to an even greater turbulent viscosity gradient. The predicted value of the boundary-layer height is also much higher than expected and the Ekman spiral is too slim. The higher than expected calculated friction velocity was of 0.8 m/s.

When compared with other models that had better results for the velocity profiles it may be noted that their TKE was much lower then the one predicted by this model which never truly vanishes until very high up in the atmosphere. These effects were also noted by Detering and Etling (1985), Duynkereke (1988) and others.

* *

Just like the previous model the k-ϵF is also sensitive to the model height. The turbulent viscosity decreases after reaching a maximum that is nonetheless much higher than it should be. After reaching a minimum value (far above the represented region) the viscosity then increases again in an unbounded manner like in the previous model. However the viscosity is now generally lower than before. The ABL height is still too deep when compared to the Leipzig wind profile. After altering the parameters a decrease in the TKE can be seen earlier and to a value closer to zero than before which is more akin to the models that yielded a better fitting to the experimental data. The TKE dissipation also has a shape that is closer to the one of k-ϵ-ℓX where a sudden decrease takes place at the ABL height, even though in the present case this is noted at a much higher altitude (not represented). Overall the turbulent quantities have a general shape that is in accordance with experimental data but out of proportion. This can also be seen in the friction velocity of 0.81 m/s, this is slightly higher than in the previous model.

The fact that the turbulent viscosity is closer to experimental data leads to better results in velocity with a slightly broader Eckman spiral.

Both Detering and Etling (1985) and Freedman and Jacobson (2002) attempted at different times to parametrize the k-ϵ model to the neutral atmosphere, however from the obtained results from models k-ϵD and k-ϵF (as well as those from other authors that tried other parameterizations) it seems that the k-ϵ is not a good model for this theoretical atmosphere and that further attempts to find a better parameterization are fruitless. Instead an alteration to the ϵ equation or completely different models should be looked into as has already been suggested by Duynkereke (1988) or Detering and Etling (1985).

* *

Regarding the ℓB model there is, in fact, a good correlation between the calculated and observed values of TKE dissipation. Analyzing the turbulent viscosity one may conclude that experimental and simulated results have the same shape and there is but a small deviation, when compared to previous models, from the experimental magnitude. The calculated ABL height seems to be slightly higher and this becomes more evident on inspection of the velocity profiles. Associated with the smaller turbulent viscosity close to the ground, is a greater velocity and therefore friction velocity of 0.71 m/s as well. A smaller ν_t also leads to greater velocities overall as becomes especially evident in the component perpendicular to the geostrophic wind speed. The Eckman spiral achieved better results but it over-predicted the angle that the wind speed close to ground made with the geostrophic wind speed.

Although ℓB is a good model there is still room for improvement. The TKE dissipation is coincident with the experimental data and this could hardly be otherwise since Blackadar (1962) used the Leipzig wind profile to calibrate his model. There is, however a notable difference in the calculated turbulent viscosity that depends on the mixing length and the velocity gradient. The assumption that the mixing length used for the calculation of ϵ is the same as the one used for the calculation of ν_t is not a fact (Cuxart *et al.*, 2006) and therein may lie the discrepancy between the calculated and observed profile of the turbulent viscosity.

* *

As for the k-ℓB it provides better results for the neutral case than the previous ones. Unlike models k-ϵD and k-ϵF this one has a TKE that approaches zero much quicker thus creating a shallower ABL. This is because the TKE dissipation is greater throughout the whole domain due to its tight dependence on the mixing length. From these two parameters a more realistic turbulent viscosity can be calculated. It reaches a maximum close to the ground and then tends to zero as it approaches the ABL height. The shape and magnitude of the turbulent viscosity are in accordance with the Leipzig wind profile although it is still slightly smaller, hypothetically for the same reasons mentioned before.

* *

The last model k-ϵ-ℓX gives good results similar to the ones of the mixing length model. Xu and Taylor (1997) have apparently predicted the ϵ production correctly since it has a shape very similar to the one of the mixing length model except for the fact that it tends to zero more quickly at higher altitudes (not represented). The dissipation is however slightly stronger than in the ℓB model which could mean that some fine tuning of the $C_{\epsilon 1}$ constant would be required if a perfect match to Blackadar (1965) was desired.

Just like in k-ℓB there is a very quick decay of TKE with height and the two profiles are practically coincident throughout the domain. k-ϵ-ℓX generates an ABL slightly deeper than k-ℓB and like the previous models that used the mixing length relation it predicts higher velocities overall while the turbulent viscosity is smaller than for the experimental data. The friction velocity was very close to experimental data at 0.66 m/s.

An attempt to alter the model by using the classical standard model definition of turbulent viscosity led to no outstanding results with its friction velocity increasing to

0.68 m/s along with the ABL depth. By making it closer to the standard model, k-ϵ-ℓX departed further from the solution of Blackadar (1962). This alteration may however be an interesting one for a case where more versatility is required.

k-ϵ-ℓX maintains some of the versatility of the standard model by having two prognostic equations for the TKE and its dissipation but due to a small alteration is able to successfully simulate the neutrally stratified ABL. Other models exist that make small ajustments to the production terms, some with better or worse results like the one from Duynkereke (1988) or the one from Detering and Etling (1985).

4.2 Transient ABL Simulations

Large Eddy Simulations have proven to be quite accurate when representing turbulent quantities or time averaged parameters as was observed during an inter-comparison study in Beare *et al.* (2006). Pedersen *et al.* (2014) made several simulations using a Large Eddy Simulation (LES) model to predict the evolution of the ABL for several cases. Among these is one of special interest for this topic that has a neutral boundary layer, *i.e.* no surface heat flux but an imposed temperature gradient of 0.003 K/m starting above it, very similar to the one of the Leipzig case. On the previous section it was assumed that the profile was in a steady-state, thus the time derivative was discarded. In this one the evolution of the profile will be compared with the LES simulation of Pedersen *et al.* (2014). The initial conditions are a zero velocity gradient with $\vec{v} = \vec{G} = (10, 0)$ m/s. Since no information was given by Pedersen *et al.* (2014) regarding turbulent quantities, a constant flux layer was assumed and the relations for the SL were applied to the whole ABL, to initialize the TKE and its dissipation. The Obukhov length was fixed at infinity, the roughness height set to 0.01 m and the Coriolis parameter to 10^{-4} s$^{-}1$. The only field variable that was not initialized as in the LES results was the temperature gradient which was set to zero as in the previous section. This was done so that its influence could be kept from influencing the results, thereby allowing a clearer analysis of the effects of the relevant equations for the neutral case.

4.2.1 Results

After running the simulations for all five previously described models during a period of 32 hours the results were compared with the LES model. In order to do this Hovmöller diagrams were made representing the source term of the momentum equations. This is directly proportional to the difference between geostrophic and local wind speed. Despite the deficiencies of the rainbow palette (Stauffer *et al.*, 2015), this colormap was chosen so as to allow for a better comparison of the present results with the LES model results of Pedersen *et al.* (2014). The ABL height was defined as the point where the shear stress reaches 5% of its surface value so that an objective analysis of its evolution could be made. The Hovmöller plots are represented in Figure 4.4, the reference case by Pedersen *et al.* (2014) in Figure 4.5 and the ABL height in Figure 4.6. The values of u_* and maximum wind speed for the last time step are presented in Appendix B with the respective errors.

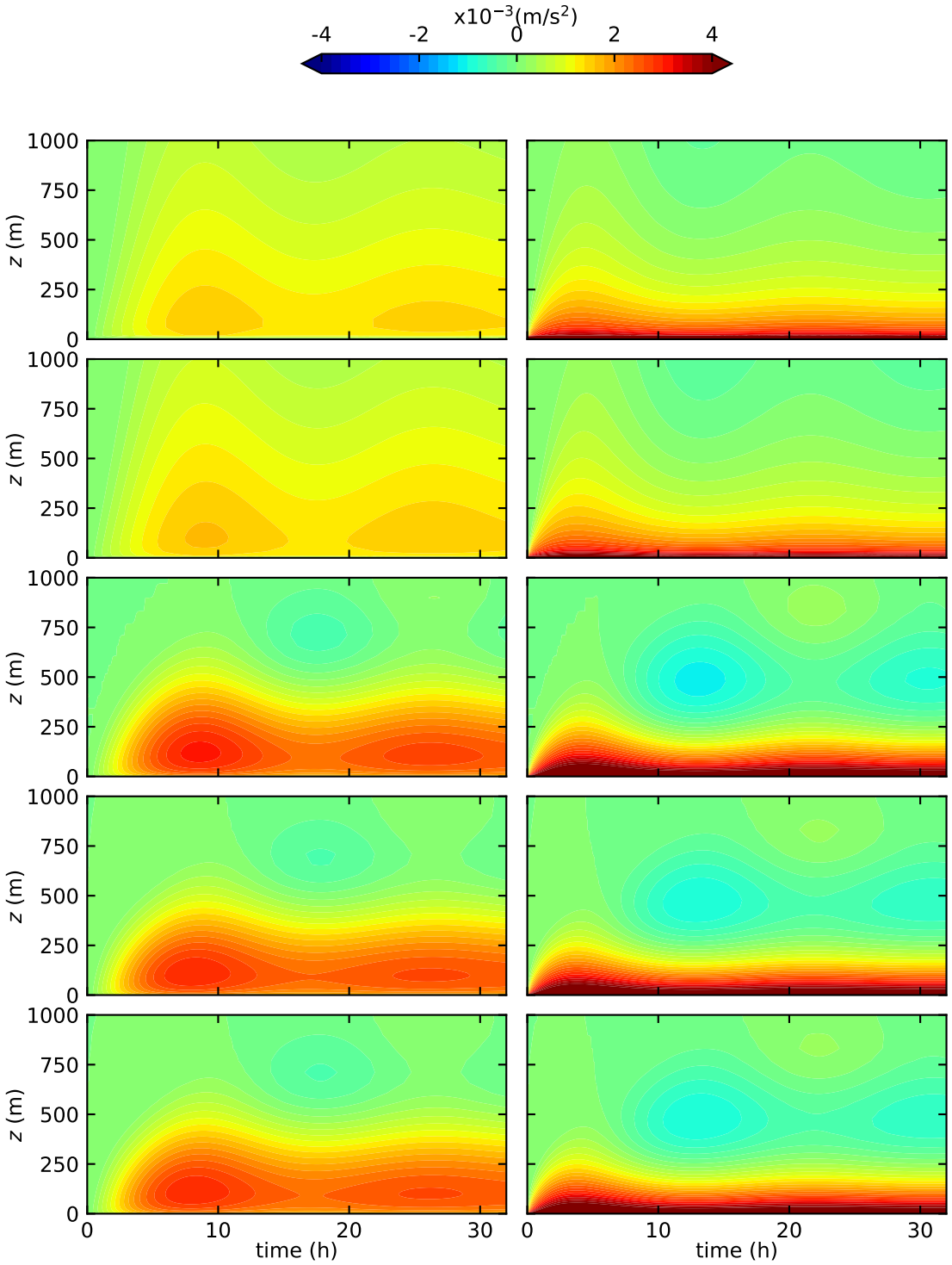

Figure 4.4: The source term for the two momentum equations given by $f(v_y - G_y)$ for the equation in the x direction (left column) and $f(G_x - v_x)$ for the equation in the y direction (right column). The models are as described from top to bottom: k-ϵD, k-ϵF, ℓB, k-ℓB, k-ϵ-ℓX.

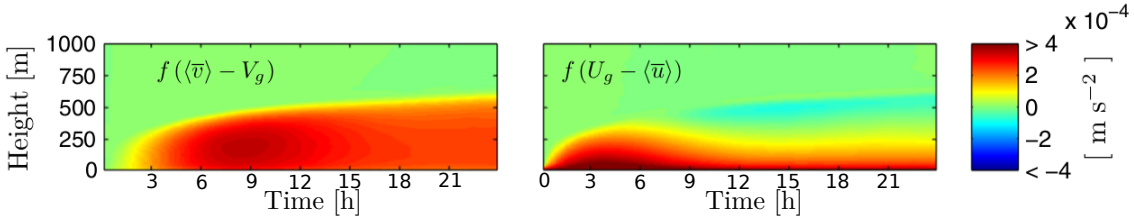

Figure 4.5: The results from the reference LES results presented with the same arrangement as in Figure 4.4. Note: adapted from the original figure in Pedersen *et al.* (2014).

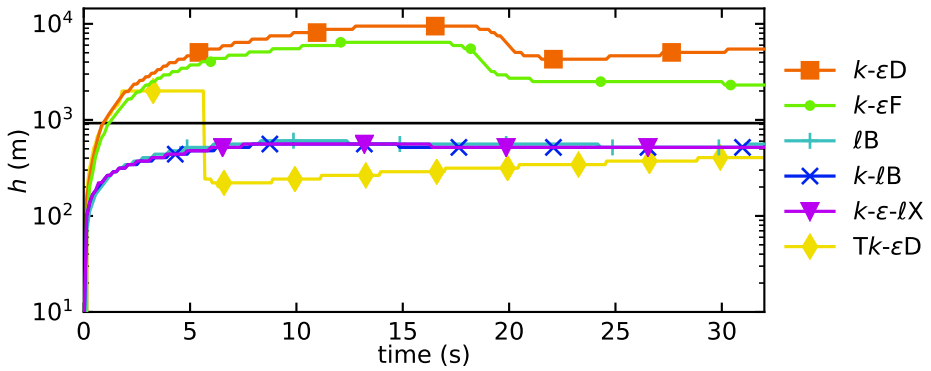

Figure 4.6: The ABL height for all models as previously defined. The Tk-ϵD model repeats the k-ϵD model but considering the effects of a weak temperature gradient (please refer to Section 4.2.3). The horizontal line is set at the theoretical ABL height of $0.25\,u_*/|f|$ with $u_* = 0.37$ as in Pedersen *et al.* (2014).

4.2.2 Analysis

Regarding the performance of the k-ϵD model, during the first four hours the wall shear stress leads to an abrupt decrease in speed that weakens with height. After five hours the wind starts to rotate with height forming a spiral. This can be seen by the increase of the velocity v_y in the lower part of the ABL. Its magnitude and direction then oscillate with time. The amplitude of these oscillations becomes progressively smaller as the system tends to its steady-state. This effect can not be seen in the LES solution and may have been created by the fact that several physical phenomena are unable to be modeled by a one-dimensional model such as this one, whereas in LES the three-dimensional space allows for advection to be considered, increasing the number of transport mechanisms that promote the influence of neighboring cells, eventually suppressing oscillations.

While the LES model clearly shows a super-geostrophic wind speed starting between seven and nine hours of simulation (*i.e.* the blue shaded area in the source term for the y direction), k-ϵD was not able to replicate this effect. The profile of v_x has a shape similar to the one of its steady-state solution throughout the whole simulation time.

The Hovmöller diagram for the other direction shows a generally smaller source term then the one presented on the LES model. Akin to the steady state the k-ϵD predicts a very slim spiral. Although the height at which v_y reaches zero starts to decrease after reaching ten hours, the LES model suggests that it would increase even after the full simulation time had passed. Nonetheless, the magnitude of the source term becomes smaller after ten hours of simulation in both cases.

Although Pedersen *et al.* (2014) calculated an increasing ABL height with time, k-ϵD predicts that it should reach a maximum after 15 hours and then decrease to more reasonable values. Even after doing so its calculated magnitude of 1.5 times u_*/f is always much larger than the predicted value of 0.25 u_*/f. After decreasing it then increases slightly again.

Analyzing the Hovmöller diagrams and its oscillations with time it now becomes obvious why the temporal convergence of such a one- dimensional model is not easy. It still reaches convergence with a much smaller computational time than the much more complex LES model.

* *

The Hovmöller diagrams for k-ϵF do not differ much in shape from the first ones. The oscillations have the same frequency and the time it takes for the braking effect of the no slip condition on the ground to reach the top of the ABL is about five hours for both. This means that, when compared to the LES simulation, both models predict the evolution of the wind profile over time correctly. The shape of the profile, however, is better on k-ϵF.

Just like for the steady-state runs the k-ϵF yields slightly higher velocities in the v_y component then the first, suggesting that the Ekman spiral is broader and closer to the reference simulation.

The ABL height has a maximum just like k-ϵD, although it only goes up to 1.7 u_*/f. Afterwards it tends asymptotically to a value of 0.65 u_*/f.

* *

If turbulence does not change instantaneously then the same should apply to the turbulent viscosity, meaning that a model where turbulence can change instantaneously could lead to inaccurate results for transient simulations. Although ℓB relies on an algebraic equation that does not depend on time and therefore has no inertial term this does not seem to impact the results in a negative way. The oscillations and their maximums still occur at the same times as for the previous models. This means that the turbulent viscosity in models k-ϵD and k-ϵF was adapting to the velocity profiles much faster than the rate of change of the profiles themselves and therefore whether the inertial term was taken into account or not had no impact on the viscosity and consequently did not delay any phenomena. If the turbulent viscosity profile were to be delayed by any inertial terms this would make the first minimum (at 13 hours for the source term in the y direction) take longer to be reached since its existence is related to an increase of viscosity that leads to stronger gradients of velocity with height.

As in the steady-state simulation ℓB develops a super-geostrophic wind speed starting at the seventh and the eighth hours just like in the reference model (*i.e.* blue region in the Hovmöller diagram for the y direction source term). This leads to a spiral similar to the classical Ekman solution Arya (2001).

As for the source term in the x direction the Hovmöller diagram shows a greater magnitude of v_y than for the previous models as in the steady-state case. While the LES simulation predicts values of v_y greater than the ones calculated by models ℓB, k-ℓB and k-ϵ-ℓX, the steady-state analysis led to the conclusion that the same models generated a greater maximum of v_y than the observations from the Leipzig wind profile. It could be argued that the differences to the reference data of both the steady-state and this case should be similar. It has to be noted, however, that there is no Rossby similarity for both cases, given the different geostrophic wind speeds and roughness heights.

As far as the ABL height of the ℓB model is concerned, there is an increase as the profile starts to develop after which it achieves an approximately constant value of $0.17\,u_*/f$.

* *

Models k-ℓB and k-ϵ-ℓX yield very similar results to ℓB. The shape of the profiles is the same throughout and only their magnitudes are slightly different. Just like in the steady-state results the Ekman spiral is slightly slimmer for the k-ℓB model than the previous which results in slightly smaller speeds in the y direction. Since the differences are minimal for both the steady-state profiles and the Hovmöller diagrams it is hard to say which of these three models is closer to reality. The fact that the LES and the Leipzig data have their own uncertainties shoud also be considered.

4.2.3 The Importance of Temperature (Tk-ϵD)

The truly neutral case is practically nonexistent, especially over a period of several hours as was simulated. This is because the smallest temperature gradient will lead to important changes in the velocity and viscosity profiles. In order to show this, k-ϵD was slightly altered in order to account for a temperature gradient of 0.003 K/m as is the case in the LES simulation and the Leipzig wind profile which resulted in model Tk-ϵD.

Equation (2.18) was used to calculate the temperature in the center of the domain. For the lower boundary the heat flux was set to zero, as for the upper boundary the top node was extrapolated from the two nodes below it thus ensuring an equal heat

flux in its lower and upper faces. The buoyancy term was added to the production of TKE as is defined in (2.33), meaning that a positive temperature gradient leads to a decrease of TKE and therefore of the turbulent viscosity. The reference temperature for the buoyancy term was set so that the Brunt-Väisälä frequency given by $N = \left(\frac{g}{\theta_r}\frac{\partial\theta}{\partial z}\right)^{1/2}$ is equal to 0.01s^{-1} as was set for the LES simulation.

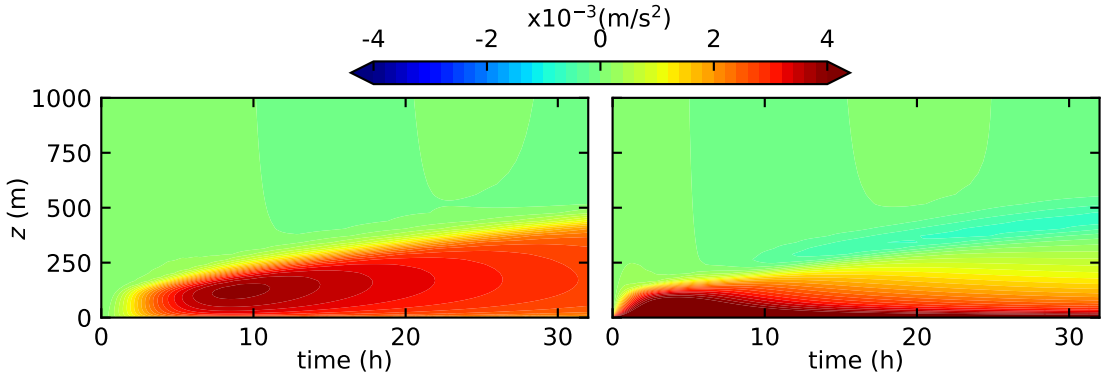

Figure 4.7: Same as Figure 4.4 for the Tk-ϵD model which takes the temperature gradient into account.

The results are clearly different from the previous models and in better agreement with the LES model results. It can be seen that the velocity defect profiles in Figure 4.7 are inhibited to grow beyond a certain height that varies over time. In fact the turbulent viscosity for the last time-step drops to a residual value at a height of 500 m due to the strong positive temperature gradient that occurs in this region suppressing the TKE as can be seen in Figure 4.8. This sort of behaviour of the ABL has been previously observed (Arya, 2001) and is termed an inversion since in the unstable case the ABL top is characterized by a positive temperature gradient, whereas below this in the mixing layer the gradients are typically zero. The position of this inversion tends to grow over time which allows the velocity profiles to develop higher. This phenomenon also happens in this simulation as can be seen from the Brunt-Väisälä frequency plot (Figure

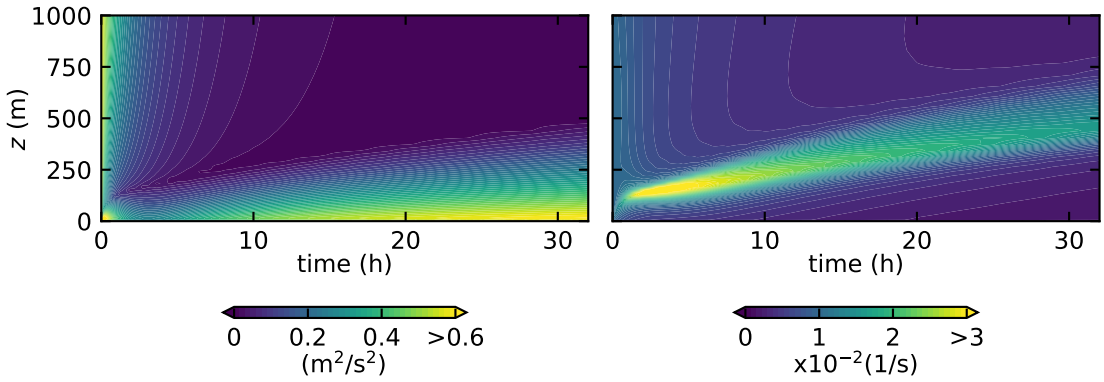

Figure 4.8: The TKE (left) and the Brunt-Väisälä frequency (right) Hovmöller plots for model Tk-ϵD.

4.8) that is proportional to the square root of the temperature gradient.

The oscillations present on the previous models still occur in this one. The super-geostrophic wind speed can also be found starting at the same time as in the previous simulations, but at a lower altitude. At all times the velocity profiles are developed at a lower height than in the LES model, suggesting that the reduction of turbulent viscosity should be happening higher up. As in the reference case the height at which v_y reaches zero keeps growing over time. The same can be said about the ABL height also plotted in Figure 4.6 that has a positive growth after the first five hours.

This growth is not always constant, since before reaching the five hours the inversion has not yet had enough time to grow and suppress all the TKE above it thus resulting a higher ν_t. The ABL height of this model actually overlaps the one from the k-ϵD during the first two hours going as high as the computational domain height, hence the plateau between 2h and 5h. The high viscosity above the inversion does not allow the velocities to reach their geostrophic speeds which in turn results in a deeper boundary-layer. At around five hours the TKE has already reached low enough values, allowing the ABL to drop to more reasonable height values.

The decrease in ν_t at the inversion cap becomes evident in Figure 4.9 where the profile of ν_t is plotted. The turbulent viscosity reaches a maximum between the ground and the ABL height and then decreases to approximately zero. After that it increases again in a manner similar to the one observed in the simulations with a zero temperature gradient. These high values of ν_t in a region of the atmosphere where the velocity gradient is zero have no impact on the velocity profile, however they are responsible for an increase of diffusivity for the temperature profile which will result in a smaller gradient for the same heat flux. On further analysis, by allowing the model to run for a longer period of time negligible values of ν_t can be achieved above the inversion as can be seen from Figure 4.10.

The Tk-ϵD was able to describe the ABL correctly up to the inversion cap with possible deviations from reality in the temperature profile after that. This shows that the analysis of the Leipzig wind profile and parameterizations for it should include the effects of temperature, at least as far as the models including the k equation are concerned. If these are not included, then the parameterizations for both k and ϵ will only be successful if their constants force it to be so artificially, which will lead to a lack of generality and theoretical basis. This supports the findings of Duynkereke (1988) suggesting that the Leipzig wind profile is not representative of the truly neutral ABL and that the effect of stability is paramount.

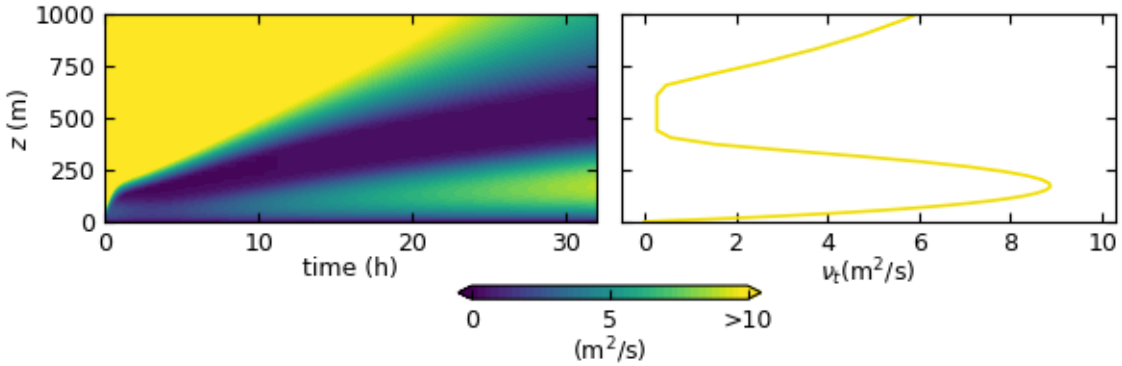

Figure 4.9: The turbulent viscosity, ν_t, Hovmöller plot for model Tk-ϵD (left) and the same variable plotted as a vertical profile for the last time step at 32h (right).

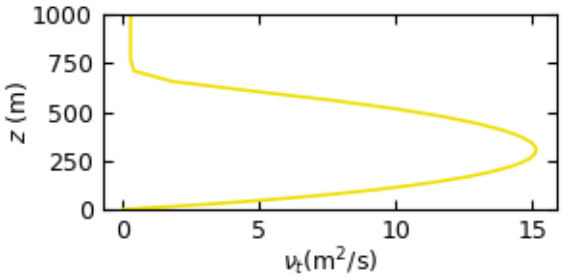

Figure 4.10: The turbulent viscosity as in Figure 4.9 (right) after a simulation time of three days.

Chapter 5

Simulation of the Stably-Stratified ABL

The Stably-Stratified ABL is simulated with variations of the previous five models. The results are presented and analyzed and a sixth model is suggested.

The LES simulation study by Beare *et al.* (2006) was used to compare several single column models during the GABLS1 program. The first GEWEX ABL Study (GABLS1) started as an intercomparison of LES models focusing the simulation of the ABL under stably-stratified conditions, based on the simulations by Kosovic and Curry (2000) of the quasi-steady ABL under a constant surface cooling rate and geostrophic wind conditions. A total of 11 models participated in this benchmark (Beare *et al.*, 2006) and its results were used as reference to a new benchmark of single-column ABL solvers (Cuxart *et al.*, 2006), consisting of 21 computer codes whose turbulence modelling ranged from first-order to two-equation higher-order schemes.

The initial and boundary conditions are well described in Cuxart *et al.* (2006) so this case will be used for comparison with the present models. The conditions were:

- Latitude: 73^o N,
- Computational domain height: 400 m,
- Geostrophic wind: $\vec{G} = (8, 0)$ m/s,
- Initial wind speed: $\vec{v} = \vec{G}$ m/s for the whole domain except on the ground,
- The potential temperature is equal to 265 K up to 100 m and then increases with a lapse rate of 0.01 K/m,
- The TKE follows $0.4(1 - z/250)^3$ m^2/s^2 up to 250 m and then retains its last value,
- The wall potential temperature follows $265 - 0.25\,t$ K with time t in hours,
- The roughness height is 0.1 m for both momentum and heat,
- The simulation time spans nine hours.

Some conditions were not met such as the grid that was not altered to a uniform formulation since this would increase computation time and decrease accuracy. The time step of 10 s led to divergence in certain cases so it was changed to 2 s.

5.1 Description of the ABL Models

All models required some modifications so as to be able to represent the stable case as accurately as possible. This includes first and foremost the introduction of a temperature transport equation since it is the basis from which most models account for stability.

Regarding the lower boundary conditions the $\phi_{m,h}$ functions are used to modify the logarithmic-profile law, thus requiring the calculation of the Obukhov length scale. Since the temperature is imposed this is done using an iterative method:

The bulk Richardson number close to the wall is defined as

$$\mathrm{Rb} = \frac{g}{\theta_0} \frac{z_1(\theta_1 - \theta_w)}{v_{x1}^2 + v_{y1}^2} \tag{5.1}$$

and from the SL relations it is known that $\Delta\theta = \theta_* \theta_1^+$ and $\sqrt{v_{x1}^2 + v_{y1}^2} = u_* u_1^+$, as in equations (2.53) and (2.54). Bearing the equation for the Obukhov length in mind (equation (2.45)) it can be rewritten as

$$\mathcal{L} = \frac{z_1}{\kappa \mathrm{Rb}} \frac{\theta_1^+}{u_1^{+2}}, \tag{5.2}$$

where the θ^+ and u^+ functions depend on $\mathcal{L}$ and z which is why an iterative solution is required. The secant method was used to find the root of equation (5.2). Knowing $\mathcal{L}$ both friction velocity, u_*, and friction temperature, θ_*, are calculated from SL relations.

k-ϵ**Ds**

Besides the afforementioned differences this model retained its previous characteristics (vide Section 4.1.1. The constants used for the TKE and its dissipation remained same. This means both the mechanical and buoyant production terms are affected by $C_{\epsilon 2}$ unless if the temperature gradient is positive, in this case only the mechanical term is taken into account in the dissipation equation as described in section 2.3.1.

k-ϵ**Fs**

This model is the same as the k-ϵDs except for the constants used in the ϵ equation which were changed to match the ones from Freedman and Jacobson (2002) as used in the neutral k-ϵF.

ℓ**Bs**

The turbulent viscosity for this model was calculated from a single mixing length using equation (2.39) similar to the neutral case. The main difference lies in the fact that the algebraic equation for ℓ is now an adaptation of the one from Blackadar (1965) to the stable case. As is evidenced by the ϵ equation in the k-ϵ model, the TKE dissipation is dependent on the temperature gradient, implying that its mixing length also depends on it (a higher ℓ leads to a lower ϵ). In order to account for this dependence several solutions have been presented, *e.g.* Holt and Raman (1988). A formulation first suggested by Djolov (1973) makes use of the SL ϕ_m function. Even though it is debatable whether it is acceptable that the mixing length in the core of the ABL be modelled using SL relations,

it is nonetheless a better approximation to the stratified case than one where it is simply assumed that the mixing length is the same for the neutral or the stable case.

The mixing length in this model is calculated as

$$\ell = \frac{\kappa z}{\phi_m + \frac{\kappa z}{\lambda}} \tag{5.3}$$

where $\lambda = 4 \times 10^{-4} \cdot G/f$.

k-ℓ**Bs**

This k-ℓ model required an alteration to its mixing length. As was noted previously, the alteration suggested by Djolov (1973) is not suitable for the region outside the SL, therefore another equation was used. This one was proposed by Duynkerke and Driedonks (1987) and requires the evaluation of three mixing lengths where the smallest is afterwards chosen. The first depends on the height of the ABL and is the previously used λ, but using a factor of 2.7×10^{-4} as in Blackadar (1962) and described in section 2.3.2. A second one depends on the distance from the ground and is given by an expression similar to the one from Blackadar (1962) like in equation (5.3). Finally one that is a function of the Brunt-Väisälä frequency and the TKE to account for stability,

$$\ell_s = c_s \frac{\sqrt{k}}{N}$$

where c_s is given a value of 0.36.

The TKE is calculated as in models k-ϵDs and k-ϵFs while its dissipation uses the relations presented for the k-ℓ model in the neutral case. Likewise the turbulent viscosity is calculated from k and ℓ as before with equation (2.41).

k-ϵ-ℓ **As**

The model presented by Xu and Taylor (1997) was tuned to the neutral ABL, which is expected to hinder its performance. The fact that its mixing length used the original expression from Blackadar (1962) also points to this. Instead another model proposed by Apsley and Castro (1997) that makes use of all three parameters – k, ϵ and ℓ– was chosen for this case.

The main purpose of Apsley and Castro (1997) when developing the model was to have a limited length-scale model where both production and destruction of ϵ would cancel one another out when the maximum mixing length was reached. The ϵ equation can be seen as a way of defining the mixing length since both quantities are directly related through equation (2.42), thus imposing a limit on ℓ is the same as imposing a limit on ϵ. The modification to the ϵ equation is such that it is no different from the k-ϵ equation (2.36) when very close to the ground and progressively reaches the point where production and destruction cancel out so that

$$\frac{D\epsilon}{Dt} = \nabla \cdot \left(\frac{\nu_t}{\sigma_\epsilon} \nabla \epsilon\right) + \left(C_{\epsilon 1} + (C_{\epsilon 2} - C_{\epsilon 1}) \frac{\ell}{\ell_{max}}\right) \mathbb{P} \frac{\epsilon}{k} - C_{\epsilon 2} \frac{\epsilon^2}{k} \,. \tag{5.4}$$

From the SL relations, making use of the MOST, the maximum mixing length becomes $\ell_{max} = \mathcal{L}\,\kappa/\beta_{ms}$ and the local mixing length is

$$\ell = \frac{\kappa z}{1 + \beta z/\mathcal{L}} \,. \tag{5.5}$$

Having ϵ the TKE is calculated according to equation (2.33) and the turbulent viscosity to equation (2.32) like in the k-ϵ model. Apsley and Castro (1997) have defined a set of constants to be used in their model very similar to the ones given by Jones and Launder (1972), however for k-ϵ-ℓAs another set of constants will be used. This should not be a problem according to Apsley and Castro (1997) since the model is general enough and is expected to yield better results given that the standard model is tuned for common engineering applications and not the ABL. Thus the constants suggested by Duynkereke (1988) will be used as described in Section 4.1.1.

k-ϵ-PrV

All previous models assumed that the Prandtl number relating the turbulent viscosity to the thermal diffusivity was constant throughout the whole height of the ABL and independent of stability. There is no reason why this should be so and therefore some parameterizations for this quantity have been developed. The Prandtl number is important to define the buoyant production of TKE which appears in the k and ϵ equations as well as for the temperature equation and is therefore especially important for the stable ABL. Venayagamoorthy and Stretch (2010) have suggested a paramaterization for the Prandtl number based on relevant length scales and the Richardson number such that

$$\mathrm{Pr} = \mathrm{Pr}_n \exp\Big(-\frac{\mathrm{Ri}}{\mathrm{Pr}_n\,\Gamma_\infty}\Big) + \frac{\mathrm{Ri}}{\mathrm{Rf}_\infty}\,, \tag{5.6}$$

where Pr_n is the Prandtl number for a neutrally stratified ABL, the one being used for all previous models, $\Gamma_\infty = \mathrm{Rf}_\infty/(1-\mathrm{Rf}_\infty)$ and Rf_∞ is the upper limit for the flux Richardson number. Venayagamoorthy and Stretch (2010) then tuned the relevant constants based on DNS simulations obtaining $\mathrm{Rf}_\infty = 1/4$ and $\Gamma_\infty = 1/3$. As for the Prandtl number for neutral stratification the previously used value of 0.95 will be used to maintain coherence.

This parameterization of the Prandtl number was applied to the k-ϵDs model and no equations or constants were altered.

5.2 Results

The GABLS1 intercomparison used the average quantities of several LES models as a reference. Akin to Cuxart *et al.* (2006) the LES results were plotted alongside the simulation results for the stable case as gray areas when the confidence interval was given to show the dispersion of the LES models or a single gray line if the average was given. The values of u_*, maximum windspeed and ABL height for the last time step are presented in Appendix B with the respective errors.

5.3 Analysis

The k-ϵDs model was able to predict the turbulent viscosity with good accuracy when compared to the other models. This led to a good prediction of the wind speed. The momentum flux should reach zero by 200 m or lower, however this was not the case. A likely reason for this is the lower limit set on ν_t. As may be seen by analyzing the profile of ν_t in Figure 5.2 the turbulent viscosity is constant from 150 m upwards, and though

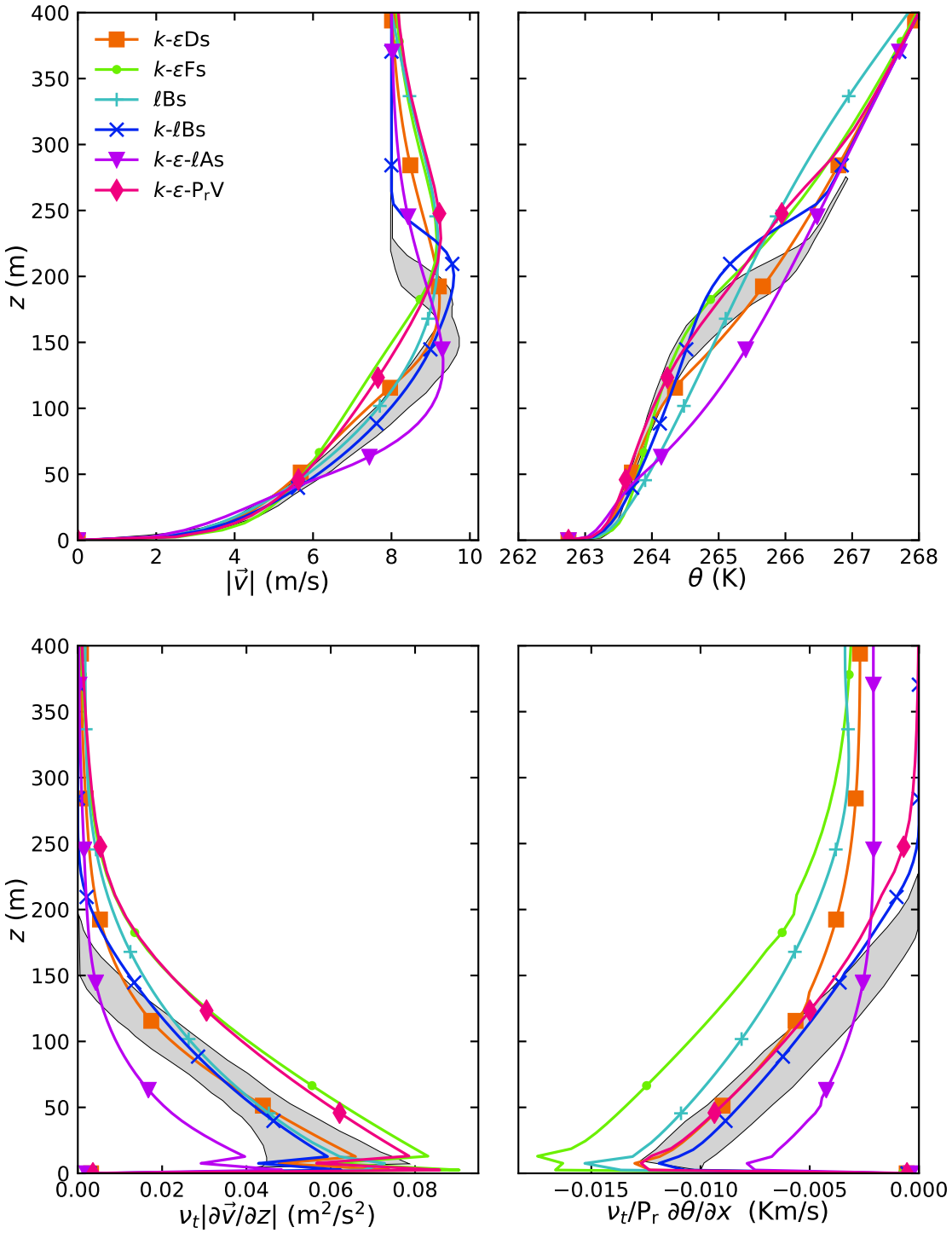

Figure 5.1: Variables for the ninth hour of simulation plotted against the domain height. The magnitude of the wind speed (upper left); the temperature profile (upper right); the momentum flux (upper right); the heat flux (lower right).

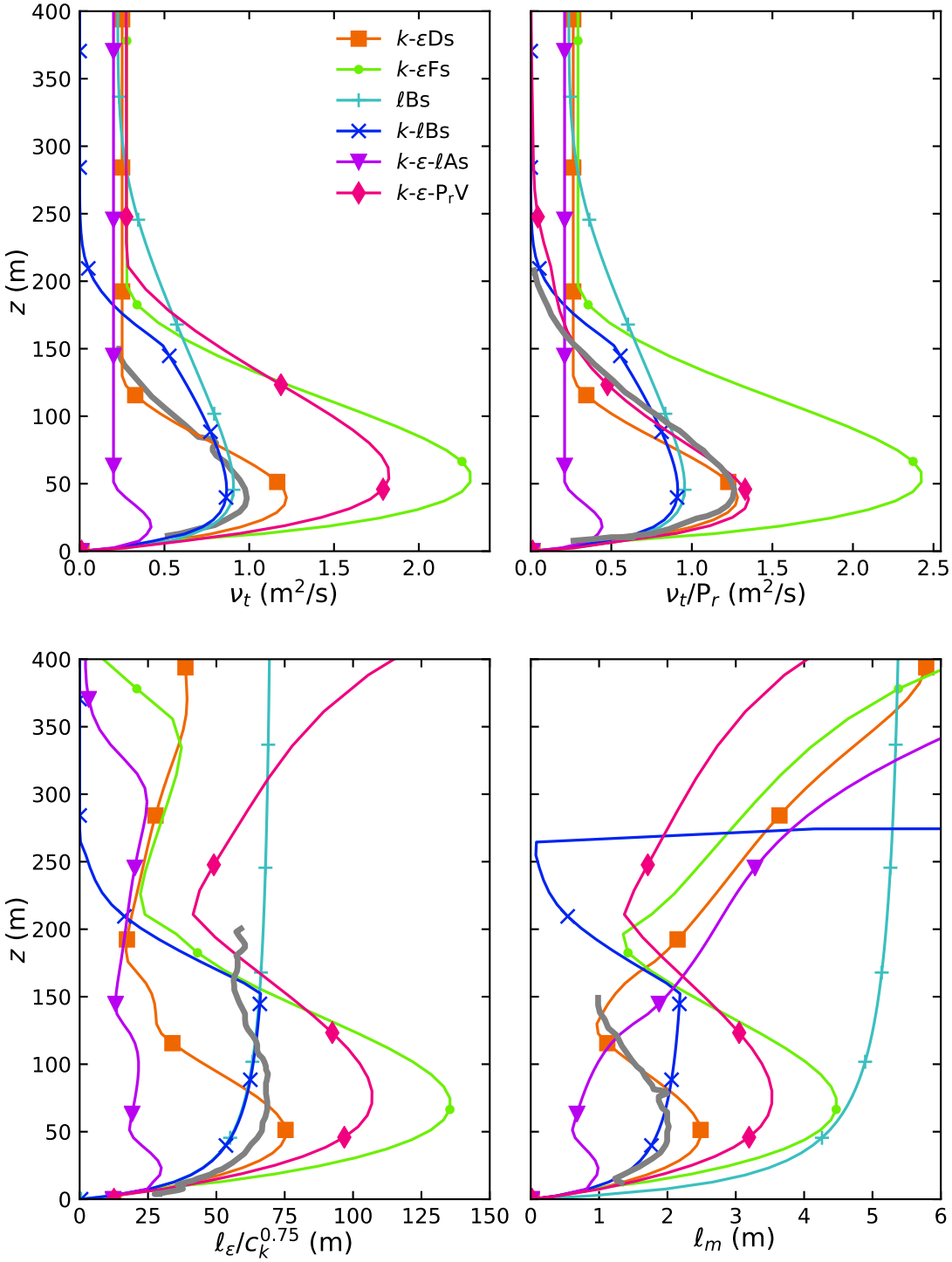

Figure 5.2: Profiles of turbulent length scales arranged as in Figure 5.1. The dynamic viscosity (upper left); the thermal diffusivity (upper right); the dissipation length ℓ_ϵ given by $c_k^{0.75}\,k^{1.5}/\epsilon$ was divided by $c_k^{0.75}$ so that different values of c_k still allowed for a comparison between models (lower left); the mixing length ℓ_m given by $\nu_t/k^{0.5}$ (lower right). For models ℓBs and k-ℓBs ℓ_ϵ was plotted as ℓ and likewise for ℓ_m in the first case.

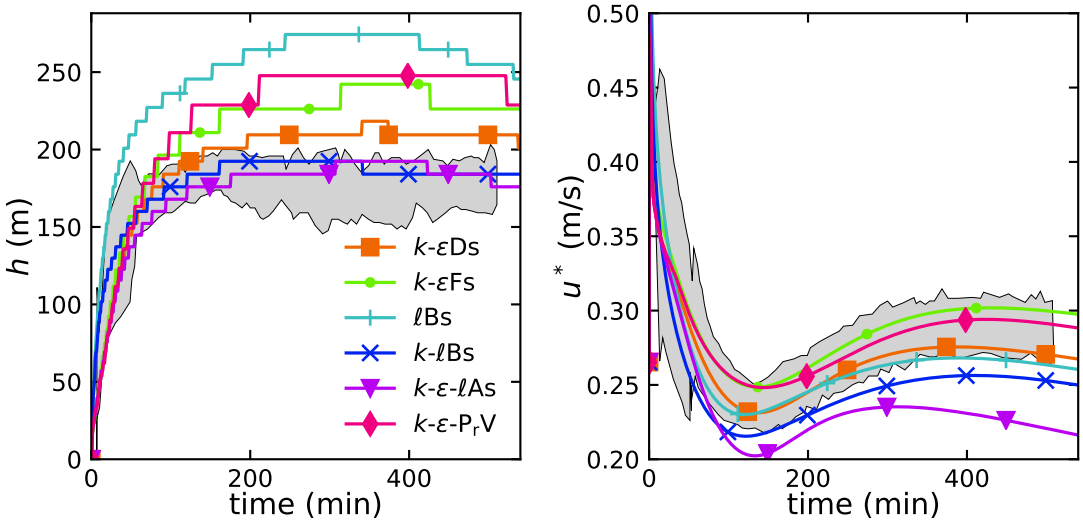

Figure 5.3: The ABL height (left) and the friction velocity (right) are plotted for the whole simulation time of 9h. The six models for the stably-stratified ABL are represented.

some models naturally predict a stabilization of ν_t this may be an artificial behaviour due to the limiters. This may be confirmed with a simple analysis of the results, a value of $\nu_t = 0.25\,\mathrm{m^2/s}$ was obtained for the first node which was precisely the value of ν_t in the upper part of the profile. Given more freedom the model would be allowed to predict smaller values of ν_t and thus better results for the momentum flux and wind speed would be obtained. On the other hand the lower limit for k-ℓBs model was of ten times its molecular viscosity, which allowed it to reach lower values.

Directly connected to the excessive momentum flux on the upper part of the domain is a higher than expected ABL height (Figure 5.3). As for the prediction of quantities near the ground, the values of u_* show a good agreement with the LES results.

In a similar manner to the momentum, the heat flux was not allowed to reach zero because of the artificial lower limit on ν_t. If this limit were to be removed, some parameterization would have to be made regarding the Prandtl number nonetheless. From a visual analysis alone it is possible to infer that the relation ν_t/ν_h is different for the LES results and the k-ϵDs model.

Analyzing the mixing length ℓ_m it can be concluded that the TKE is being predicted quite well, at least until 150 m where the limiter for ν_t sets in. As for ℓ_ϵ it reaches an approximately constant value from 150 m upwards which is consistent with the LES data as well as the ℓBs model, shich means that it is similar to the Leipzig wind profile used for the parameterization of Blackadar (1962). The value to which it tends, however is slightly lower than it should be. The increase in ℓ_m from 150 m upwards can be traced back to the limit of ν_t. Given that this parameter is restricted by a lower limit, ℓ_m will necessarily increase as the TKE decreases. This is because $\ell_m = \nu_t/k^{0.5}$ and ν_t is not allowed to change.

* *

The k-ϵFs model gives values of ν_t that are too high, therefore the calculated ratio of k^2/ϵ is equally high as can also be seen from the ℓ_ϵ profile in Figure 4.2. This shows the importance of parameterization constants and the ϵ equation on the prediction of ABL

flows. The cause for the discrepancy between the k-ϵDs and the k -ϵFs models can not be ascribed to one particular constant. The fact that k-ϵFs predicted a smaller turbulent viscosity in the neutral cases than k-ϵDs, as opposed to this case, shows that differences in results are dependent on flow conditions.

One possible cause for the too high ratio of k^2/ϵ (proportional to ν_t) could be the production of ϵ which is tuned by $C_{\epsilon 1}$. This constant is lower in k-ϵFs which leads to a lower production of TKE dissipation and thus a higher ratio of k^2/ϵ. This is mere speculation but would be a good starting point to study the effect of these constants on the model by parametric testing and analyzing its effects on the solution. Although the model is not usable as it is for the the stable ABL the general shape of the profiles is good and applying other values for the constants within the ranges suggested by Freedman and Jacobson (2002) might lead to good solutions.

* *

The results of the ℓB model do not differ much according to the boundary conditions due to the fact that the expression for the turbulent viscosity depends only on a single parameter and height. For this reason the profile of ν_t and wind speed are similar to the ones of the neutral case. The fact that the temperature has no effect on the turbulent viscosity leads to a much deeper ABL. In the other models ν_t is destroyed by the inversion cap at a lower altitude, which in turn leads to an accentuation of the temperature gradient and the two phenomena feed back and forth into one another. The ℓB model is unable to represent this.

Although the ℓB model should be able to predict quantities in the SL well, incorrect predictions of speed and temperature above it lead to incorrect calculations of these quantities in the SL, *e.g.* the Obukhov length requires the temperature in the first node whose temperature is affected by diffusion to the second one. Errors in the second node would thus lead to errors in the Obukhov length which would lead to errors in ϕ_h which would lead to errors in ℓ and so on. Thus the fact that a model is suitable for the SL is only true if the values above it are calculated correctly, eventually by another model. Such explains why even u_* has values that depart from the gray confidence-interval area of the LES models.

* *

The k-ℓBs model was able to correct the mixing length from the previous model by choosing ℓ_s between the inversion and the top of the domain, as can be seen in the ℓ_ϵ profile. This and the fact that the turbulent viscosity was allowed to reach much lower values than the previous models led to a prediction of the wind speed that is almost coincident with the LES predictions. The inversion is slightly higher than it should be however which leads to the slight deviation of ν_t and consequently of the wind speed. The inversion cap would most likely be lowered if the value of c_s was decreased, but that alone would not be enough since it is probable that c_s depends rather on the conditions of stability.

Duynkerke and Driedonks (1987) explain how the value of c_s was chosen according to a relation involving Ri and Rf for which they chose the critical value of 0.3 and thus arrived at $c_s = 0.36$. If instead of having c_s fixed for the whole domain it was made to depend on the Richardson numbers (not the critical ones) better results could eventually be obtained.

The ABL height is well predicted even though the inversion is slightly higher than it should be.

There are still some deficiencies in the k-ℓBs model. The turbulent viscosity has a kink at about 150 m, the point where the transition is made to the ℓ_s length. A function that would smoothen this transition could be beneficial.

The abrupt increase of ℓ_m can be ascribed to k reaching zero while ν_t reaches its lower limit of ten times the molecular viscosity.

* *

The k-ϵ-ℓAs model has successfully limited the maximum dissipation length, indirectly limiting the minimum ϵ value. This limitation was too stringent for this case where the mixing length should have reached higher values. The high TKE dissipation led to very small values of TKE and thus of turbulent viscosity.

The effect of the lower limit for the turbulent viscosity is more important in this case since it is of the same order of magnitude as its maximum. This limit is reached at a very low altitude of 50 m which leads to a very low inversion cap, that is also very weak due to the low turbulent viscosity. This resulted in a velocity profile that was not able to develop correctly within the small and more viscous region. From 50 m upward all parameters are subjected to a constant ν_t and an odd velocity profile which makes it impossible for these quantities to match the LES model results unless by coincidence.

Possible solutions for the k-ϵ-ℓAs model include: reducing the lower limit of ν_t or applying one to k instead, trying different parameterizations for the mixing length such as the one used in k-ℓBs.

* *

The turbulent Prandtl number calculated for the k-ϵ-PrVs led to a decrease of the thermal diffusivity which in turn resulted in a smoother profile of θ without a clear cap. The k-ϵ model computes a too deep boundary-layer with an ever increasing turbulent viscosity if no inversion is present, as was concluded in Chapter 4. Since there is no cap limiting the size of the ABL, ν_t is allowed to reach very high values. The overall higher Prandtl number also means that the buoyant production – in this stable case, destruction – is weaker and therefore it becomes even harder for an inversion to be created, as was seen in the ℓBs model where no coupling at all was present between temperature and viscosity.

The thermal diffusivity is decreased by the Prandtl number when according to the LES results it should be increased relative to the turbulent viscosity. There is certainly a discrepancy between the parameterization of Venayagamoorthy and Stretch (2010) and the results of the LES intercomparison, since Ri is greater than zero throughout the whole ABL, then $\mathrm{Pr}/\mathrm{Pr}_n$ should be greater than one according to equation (5.6). The decrease in thermal diffusivity between 150 and 200 m is well portrayed by this model since the Prandtl number tends to infinity in this region. The reason for this is the equally infinite Ri due to the absence of shear stress in this part of the atmosphere.

Chapter 6

Conclusions

A numerical solver for the atmospheric boundary layer based on single-column modelling was developed to analyze turbulence parameterizations for the stable and neutral atmosphere.

A total of 7 turbulence models were investigated, namely a simple mixing-length diagnostic equation, a one-equation k-ℓ model and two-equation k-ϵ and k-ϵ-ℓ formulations. To evaluate their performance, two relevant reference case studies in the technical literature were considered: the (assumed) neutrally-stratified Leipzig wind profile and the LES results from the GABLS1 model-intercomparison, focusing on a quasi-stationary stably-stratified ABL. Additionally, the LES results of Pedersen et al. (2014) were used as reference to study the effect of static-stability on the transient evolution of a neutral ABL.

The k-ϵ models predicted a very high TKE which did not vanish until very high up in the atmosphere. This created an excessive viscosity that led to a very deep boundary layer. Although a different paramaterization from the one initially used was able to lead to better results, both were unable to reproduce the Leipzig wind profile case. The cause for this was the disregard for the temperature gradients that are relevant even under neutral stratification. It was shown that the analysis of the Leipzig wind profile and parameterizations for it should include the effects of temperature, at least as far as the models including the k equation are concerned. When these were not included, the parameterizations were successful only if their constants forced it to be so artificially, which would lead to a lack of generality and theoretical basis as was done previously by Detering and Etling (1985). The reasons for this were the creation of an inversion cap that is important for the suppression of TKE.

A mixing-length model was also tested having shown very good results for the neutral atmosphere. A possible reason for the small discrepancies observed was the assumption that the mixing length used for the calculation of ϵ was the same as the one used for the calculation of ν_t. This was not necessarily true and thus more than one length scale would be necessary. It was also observed that this model was unable to simulate the growth of the boundary-layer correctly since it did not account for the effects of the temperature inversion at its top. The mixing length model had a temporal evolution that was similar to the ones of other models even though it did not have any time-dependent terms for the prediction of viscosity. This suggests that the inertial terms of viscosity had a small impact on all simulations. The mixing length model performed poorly when predicting the stratified case even though parameterizations

including some effects of temperature were used.

A k-ℓ model was then used, having performed quite well in the neutral case. The reason for this was that the mixing length used was able to predict the TKE dissipation better than the ϵ equation used in other cases. For the stratified case an alteration had to be made to the mixing length parameterization which included local quantities. This allowed it to perform satisfactorily even in the stable case. It was proposed that one of the constants used for calculating the mixing length would be made dependent on the local Richardson number, thus allowing for a better prediction of the inversion cap, whose prediction was previously inaccurate.

A model proposed by Xu and Taylor (1997) was tested having predicted the neutral case quite well due to the use of a mixing length for the calculation of the TKE dissipation. Some alterations to the model led to no remarkable differences in the results.

For the stable case a limited length scale model proposed by Apsley and Castro (1997) predicted a very low turbulent viscosity and was thus unable to predict any other quantity correctly. The cause for this could have been either a lower limiter that was imposed on ν_t or a flawed prediction of the maximum length scales.

Lastly an alteration was made to the k-ϵ model to include the effects of a variable Prandtl number. This resulted in a smoothened temperature profile with no discernible cap that hindered the bottom surface-layer profile due to exaggerated turbulent viscosity values.

Proposals for Future Work

The models for the ABL are still inaccurate and further effort has to be put into finding better solutions. Those presented in this work suggest that in light of the effects of the inversion cap on the neutral ABL the k-ϵ model should be reevaluated under different conditions to better understand how accurate and general it is. Ideally a parametric study should be carried out.

As far as the variation of the turbulent Prantl number is concerned, some investigation is required and other parameterizations that take the Richardson number into account should be tested. Different solutions or measurements could also be used so as to understand the discrepancies between the GABLS1 reference and the turbulent Prandtl number calculated using the relation given by Venayagamoorthy and Stretch (2010). Similarly more work has to be done regarding the limited length scale k-ϵ model proposed by Apsley and Castro (1997) for which other parameterizations for the mixing length should be considered. The k-ℓ model has shown great potential for both the neutral and stable case as long as the mixing length is well predicted and further work could include implementing a variable c_s dependent on the Richardson number to improve the prediction of the height of the inversion cap. Lastly all models could be tested in a convective boundary layer to evaluate their range of application. This may be done by comparing them with the GABLS2 full diurnal cycle.

Appendices

Appendix A

Choice of Mesh and Time-Step

The discretization is an approximation that leads to an error between the practical and theoretical solutions. In order to make sure that this error is negligible model 1 was run with different levels of discretization regarding both time and space. The GABLS1 conditions were used with a domain size of 1 km. Some characteristic quantities are compared for the ninth hour in the following table where the previously undefined $\Delta\alpha$ is the angle between the geostrophic and the lower boundary wind speeds.

Table A.1: Analysis of the influence of the discretization on results. $n-1$ is the number of cells used.

-	$\Delta t = 2$ s			$\Delta t = 1$ s
$n-1$	25	50	100	50
u_* (m/s)	0.265	0.267	0.267	0.267
L (m)	110	113	113	113
$\Delta\alpha$ (^{o})	35.2	35.8	36.0	35.8
$\mathtt{max}[\vec{v}\|/\|\vec{G}\|]$	1.15	1.15	1.15	1.15

As is apparent the error for using a mesh of 50 cells does not justify the usage of a finer one so this value was used for all calculations. The same can be stated about the time-step used for which a value of 2 s was chosen.

Appendix B

Other Results

The following table presents comparative results for all models. The errors are relative to the respective reference simulations or measurements, *i.e.* the Leipzig wind profile (Mildner, 1932) for the steady state (ss) simulations, the LES simulation n_{02} from Pedersen *et al.* (2014) for the neutral case transient (t) simulations (includes Tk-ϵD), the GABLS1 reference LES simulations presented by Beare *et al.* (2006) for the stratification simulations. The error of a general variable ϕ when compared with its reference was calculated as $\varepsilon_\phi = (\phi - \phi_{ref})/\phi_{ref}$.

Table B.2 then summarizes several parameters from all models.

Table B.1: Results of relevant quantities for all models. ε_ϕ is the error of variable ϕ compared to the reference displayed in **Bold** given as a percentage. (t) stands for transient and (ss) for steady-state.

Neutral (ss)	u_* (m/s)	ε_{u_*}	$\mathtt{max}[v_x]$ (m/s)	ε_{v_x}	$\mathtt{max}[v_y]$ (m/s)	ε_{v_y}
k-ϵD	0.80	22.0	18.00	3.2	2.94	32.03
k-ϵF	0.81	24.9	18.16	2.3	3.07	29.20
ℓB	0.71	9.0	18.78	1.0	5.08	17.28
k-ℓB	0.64	1.2	18.77	0.9	5.05	16.74
k-ϵ-ℓX	0.66	1.7	18.76	0.9	5.04	16.35
Leipzig	**0.65**	-	**18.59**	-	**4.32**	-
Neutral (t)	u_* (m/s)	ε_{u_*}	$\mathtt{max}[\lvert\vec{v}\rvert]$ (m/s)	$\varepsilon_{\lvert\vec{v}\rvert}$	-	-
k-ϵD	0.35	4.9	10.26	6.5	-	-
k-ϵF	0.36	3.0	10.37	7.6	-	-
ℓB	0.33	11.4	10.83	12.4	-	-
k-ℓB	0.30	17.7	10.77	11.8	-	-
k-ϵ-ℓX	0.31	16.9	10.77	11.8	-	-
Tk-ϵD	0.34	7.6	10.78	11.9	-	-
LESPedersen	**0.37**	-	**9.63**	-	-	-
Stable (t)	u_* (m/s)	ε_{u_*}	$\mathtt{max}[\lvert\vec{v}\rvert]$ (m/s)	$\varepsilon_{\lvert\vec{v}\rvert}$	h (m)	ε_h
k-ϵDs	0.27	7.7	9.23	4.2	201	13.5
k-ϵFs	0.30	2.6	9.16	4.9	226	27.8
ℓBs	0.26	10.2	9.19	4.5	246	38.7
k-ℓBs	0.25	13.8	9.59	0.4	184	4.0
k-ϵ-ℓAs	0.22	25.4	9.32	3.2	176	0.6
k-ϵ-PrV	0.29	0.6	9.26	3.8	229	29.2
LESGABLS1	**0.29**	-	**9.63**	-	**177**	-

Table B.2: A summary of the relevant boundary conditions, discretization parameters and results for all models. The solutions are for the last time step or iteration.

Model	z_{max} [m]	Δz_{min} [m]	$n-1$ [-]	Δt [s]	z_0 [m]	f [s^{-1}]	$\lvert\vec{G}\rvert$ [m/s]	u_* [m/s]	h [m]	θ_* [K]	θ_0 [K]	N_0 [s^{-1}]	$\max k$ [m^2s^{-2}]	$\max \nu_t$ [m^2s^{-1}]
k-ϵD	1.72e+04	71.4	50	0	0.3	0.000113	17.5	0.795	6.12e+03	0	290	0	3.57	869
k-ϵF	1.72e+04	71.4	50	0	0.3	0.000113	17.5	0.814	4.1e+03	0	290	0	3.84	320
ℓB	5.73e+03	31	50	10	0.3	0.000113	17.5	0.71	1.04e+03	0	290	0	2.78	14.9
k-ℓB	2.87e+03	30.7	50	10	0.3	0.000113	17.5	0.644	1.04e+03	0	290	0	2.43	13.2
k-ϵ-ℓX	2.87e+03	30.7	50	10	0.3	0.000113	17.5	0.663	1.04e+03	0	290	0	2.53	14.2
k-ϵD(t)	1.95e+04	81	50	10	0.01	0.0001	10	0.352	5.46e+03	0	290	0	0.681	828
k-ϵF(t)	1.05e+04	43.6	50	10	0.01	0.0001	10	0.359	2.12e+03	0	290	0	0.458	283
ℓB(t)	2e+03	4.07	100[1]	10	0.01	0.0001	10	0.328	576	0	290	0	0.591	3.62
k-ℓB(t)	2e+03	8.3	50	10	0.01	0.0001	10	0.304	517	0	290	0	0.547	3.32
k-ϵ-ℓX(t)	2e+03	8.3	50	10	0.01	0.0001	10	0.308	517	0	290	0	0.556	3.47
Tk-ϵD(t)	2e+03	8.3	50	5	0.01	0.0001	10	0.336	832	0	290	0.000266	0.62	20.2
k-ϵDs	400	10.1	50	1	0.1	0.000139	8	0.267	201	0.0456	263	3.44e-06	0.394	1.22
k-ϵFs	1e+03	10.2	50	1	0.1	0.000139	8	0.297	226	0.0556	263	5.1e-06	0.487	2.3
ℓBs	400	10.1	50	1	0.1	0.000139	8	0.26	246	0.052	263	4.89e-06	0.388	0.907
k-ℓBs	400	10.1	50	1	0.1	0.000139	8	0.25	184	0.0451	263	3.45e-06	0.344	0.867
k-ϵ-ℓAs	400	10.1	50	1	0.1	0.000139	8	0.216	176	0.0345	263	2.06e-06	0.257	0.421
k-ϵ-PrV	1.5e+03	10.3	50	2	0.1	0.000139	8	0.288	229	0.0425	263	2.8e-06	0.457	1.82

[1]The mesh was refined to keep track of the discretization error, a mesh of 50 led to a negligible alteration to the results.

Table B.3: An analysis of the dependence of $\max \nu_t$ and Δz_{min}. Using the k-ϵDs model and the same conditions as for GABLS1 but with a domain height of 2 km and a time step of 2s.

Δz_{min} [m]	0.2	1	4	10	20
$\max \nu_t$ [m^{2}s^{-1}]	1.6	1.6	1.5	1.2	0.9

A dependence between the solution and the height of the first cell, Δz_{min}, was found to have some importance after having run all the simulations presented in Table B.2. This relation is not to be expected since, from a conceptual standpoint, the first node for the employed value of Δz_{min} yields a first node located at a height of 5 m. This is well inside the SL which typically represents 10 % of the ABL height. For the stable case this would mean a SL height of approximately 20 m.

In fact, for $\Delta z_{min} < 10$ m the values of $\max \nu_t$ are quite similar as can be seen from Table B.3 validating this approximation. However, for values of $\Delta z_{min} < 1$ m the size of the first cell has the same order of magnitude as z_0, making the results for these cases questionable since it should be at least one order of magnitude higher than z_0.

Bibliography

Acheson DJ. 1990. *Elementary Fluid Dynamics*. Oxford University Press, 2005 edn, ISBN 0-19-859679-0.

Apsley DD, Castro IP. 1997. A limited-length-scale k-ϵ model for the neutral and stably-stratified atmospheric boundary layer. *Boundary-Layer Meteorology* **83**: 75–98.

Arya SP. 2001. *Introduction to Micrometeorology*. Academic Press, second edn, ISBN 0-12-059354-8.

Beare RJ, Macvean MK, Holtslag AAM. 2006. An intercomparison of large-eddy simulations of the stable boundary layer. *Boundary-Layer Meteorology* **118**: 247.

Beljaars ACM, Walmsley JL, Taylor PA. 1987. A mixed spectral finite difference model for neutrally stratified boundary layer flow over roughness changes and topography. *Boundary-Layer Meteorology* **38**: 273–303.

Blackadar AK. 1962. The vertical distribution of wind and turbulent exchange in a neutral atmosphere. *J. Geophys. Res.* **67**: 3095–3102.

Blackadar AK. 1965. A single layer theory of the vertical distribution of wind in a baroclinic neutral atmospheric boundary layer. *Flux of Heat and Momentum in the Planetary Boundary Layer of the Atmosphere, Final Report* : 1–22.

Cuxart J, Beare RJ, Macvean MK, Holtslag AAM, Esau I, Golaz JC, Jimenez MA, Khairoutdinov M, Kosovic B, Lewellen D, Lund TS, Lundquist JK, Mccabe A, Moene AF, Noh Y, Raasch S, Sullivan P. 2006. Single-column model intercomparison for a stably stratified atmospheric boundary layer. *Boundary-Layer Meteorology* **118**: 273–303.

Detering, Etling. 1985. Application of the e-epsilon turbulence closure model to the atmospheric boundary layer. *Boundary-Layer Meteorology* **33**: 113–133.

Djolov GD. 1973. Modeling of the interdependent diurnal variation of meteorological elements in the boundary layer. PhD thesis, Univ. of Waterloo, Waterloo, Ont., Canada.

Duynkereke PG. 1988. Application of the e-ϵ turbulence closure model to the neutral and stable atmospheric boundary layer. *Journal of the Atmospheric Sciences* **45**: 865–880.

Duynkerke PG, Driedonks GM. 1987. A model for the turbulent structure of stratocumulos-topped abl. *J. Atmos. Sci.* **44**: 43–64.

Dyer AJ. 1974. A review of flux profile relationships. *Boundary-Layer Meteorology* **7**: 363–372.

Freedman AFR, Jacobson BMZ. 2002. Transport-dissipation analytical solutions to the e-epsilon turbulence model and their role in predictions of the neutral abl. *Boundary-Layer Meteorology* **102**: 117–138.

Högström U. 1988. Non-dimensional wind and temperature proiles in the atmospheric surface layer: A re-evaluation. *Boundary-Layer Meteorology* **42**: 55–78.

Holt T, Raman S. 1988. A review and comparative evaluation of multilevel boundary layer parameterization for first-order and tke closure schemes. *Reviews of Geophysics* **26**: 761–780.

Jones WP, Launder BE. 1972. The prediction of laminarization with a two-equation model of turbulence. *Journal of Heat and Mass Transfer* **15**: 301–314.

Kitada T. 1987. Turbulence structure of sea breeze front and its implication in air pollution transport - application of k-epsilon model. *Boundary-Layer Meteorology* **41**: 217–239.

Kosovic B, Curry JA. 2000. A large eddy simulation study of a quasi-steady, stably stratified atmospheric boundary layer. *J. Atmos. Sci.* **57**: 1052–1068.

Lettau H. 1950. A re-examination of the "leipzig wind profile" considering some relations between wind and turbulence in the frictional layer. *Tellus* **2**: 125–129.

Mildner P. 1932. Uber reibung in einer speziellen luftmasse. *Beitr. Phys. fr. Atmosph.* **19**: 151.

Pedersen JG, Gryning SE, Kelly M. 2014. On the structure and adjustment of inversion-capped neutral atmospheric boundary-layer flows: Large-eddy simulation study. *Boundary-Layer Meteorology* **153**: 43–62.

Perić M, Ferziger JH. 2002. *Computational Methods for Fluid Dynamics*. Springer, third edn, ISBN 3-540-42074-6.

Pope BS. 2000. *Turbulent Flows*. Cambridge University Press, second edn, ISBN 0-521-59125-2.

Rodi W. 1984. *Turbulence models and their application in hydraulics*. International Association for Hydraulic Research.

Royal Aeronautical Society. 1973. Characteristics of wind speed in the lower layers of the atmosphere near the ground: Strong winds (neutral atmosphere). Institutional Report Eng. Sci. Data Unit 72026, Royal Aeronautical Society, London, UK.

Stauffer R, Mayr GJ, Dabernig M, Zeileis A. 2015. Somewhere over the rainbow: How to make effective use of colors in meteorological visualizations. *Bull. Amer. Meteor. Soc.* **96**: 203–216.

Stull RB. 1988. *An Introduction to Boundary Layer Meteorology*. Kluwer Academic Publishers, ninth edn, ISBN 978-90-277-2769-5.

Veiga Rodrigues C, Rodrigues AH, Palma JMLM. 2016. Atmospheric flow over a mountainous region by a one-way coupled approach based o reynolds-averaged turbulence modelling. *Boundary-Layer Meteorology* **159**: 407–437.

Venayagamoorthy SK, Stretch DD. 2010. On the turbulent prandtl number in homogeneous stably stratified turbulence. *J. Fluid. Mech.* **644**: 359–369.

Weng W, Taylor PA. 2003. On modelling the one-dimensional atmospheric boundary layer. *Boundary-Layer Meteorology* **107**: 371–400.

Xu D, Taylor PA. 1997. An e ϵ turbulence closure scheme for planetary boundary-layer models: the neutrally stratified case. *Boundary-Layer Meteorology* **84**: 247–266.

Acknowledgements

I would like to thank my coordinator Dr. Carlos Veiga Rodrigues for his invaluable support and dedication throughout all phases of this work. For sharing his knowledge in meteorology, an area of knowledge that was practically unknown to me up to the moment when the topic for this thesis was chosen. And on that regard I would also like to thank the guidance of Prof. Fernando Pinho and Prof. Alexandre Afonso who, through their multidisciplinary knowledge and openness, enabled such a topic to be formulated and researched in the department of mechanical engineering. Besides meteorology Dr. Carlos Veiga Rodrigues also taught me Python, the language used for the computational implementation, having provided me with several pieces of older codes that were reused in this work. It was also from Dr. Carlos Veiga Rodrigues that I learned LaTeXand how to elaborate a scientific document along with many other things, more precisely tools that were all of them employed to the best of my abilities for this work. I am thankful because I know that these tools were useful not only for the present but will be, no doubt, very useful for the future.

Last but not the least I would like to thank my friends and family for their support and much needed distraction when words were turning to letters and equations becoming symbols.

It is natural and nothing natural can be evil.
-Marcus Aurelius